



U.S. Department of Housing and Urban Development
Office of Policy Development and Research



Wood Shear Walls with Corners

PATH (Partnership for Advanced Technology in Housing) is a new private/public effort to develop, demonstrate, and gain widespread market acceptance for the “Next Generation” of American housing. Through the use of new or innovative technologies the goal of PATH is to improve the quality, durability, environmental efficiency, and affordability of tomorrow’s homes.

Initiated at the request of the White House, PATH is managed and supported by the Department of Housing and Urban Development (HUD). In addition, all Federal Agencies that engage in housing research and technology development are PATH Partners, including the Departments of Energy and Commerce, as well as the Environmental Protection Agency (EPA) and the Federal Emergency Management Agency (FEMA). State and local governments and other participants from the public sector are also partners in PATH. Product manufacturers, home builders, insurance companies, and lenders represent private industry in the PATH Partnership.

To learn more about PATH, please contact:



Suite B133
451 7th Street, SW
Washington, DC 20410
202-708-4250 (fax)
e-mail: pathnet@pathnet.org
website: www.pathnet.org

Wood Shear Walls with Corners

Prepared for:

The U.S. Department of Housing and Urban Development
Office of Policy Development and Research
Washington, DC

National Association of Home Builders
Washington, DC

Prepared by:

NAHB Research Center, Inc.
Upper Marlboro, MD

Contract H-21172CA

March 2001

Acknowledgments

The NAHB Research Center, Inc., expresses great appreciation to the sponsors of this work in view of its relevance to more accurate and cost-effective design of residential light-frame housing.

The Research Center personnel involved in this work include:

Vladimir Kochkin, Shawn McKee, Principal Investigators
Jay Crandell, P.E., Technical Reviewer
Ernie Jenkins, Laboratory Support
Anthony Osborne, Laboratory Support
Kimberlee Jackson, Administrative Support

Notice

The work that provided the basis for this publication was supported by funding under a grant with the U.S. Department of Housing and Urban Development. The substance and findings of the work are dedicated to the public. The author and publisher are solely responsible for the accuracy of the statements and interpretations contained in this publication. Such interpretations do not necessarily reflect the views of the Government.

The U.S. Government does not endorse products or manufacturers. Trade or manufacturer's names appear herein solely because they are considered essential to the object of this report.

ABOUT THE NAHB RESEARCH CENTER, INC.

The NAHB Research Center, Inc. is a not-for-profit subsidiary of the National Association of Home Builders (NAHB). The NAHB has 200,000 members, including 50,000 builders who build more than 80 percent of new American homes. NAHB Research Center conducts research, analysis, and demonstration programs in all areas relating to home building, and carries out extensive programs of information dissemination and interchange among members of the industry and between the industry and the public.

Table of Contents

Acknowledgments.....	ii
1. Introduction.....	1
2. Scope and Limitations.....	1
3. Background.....	2
4. Experimental Program.....	10
4.1 Wall Construction.....	10
4.2 Test Procedure and Wall Instrumentation.....	14
4.3 Definition of the Shear Wall Performance Parameters.....	16
5. Results and Discussion.....	17
5.1 General.....	17
5.2 Failure Modes.....	22
5.3 Corner Return Response.....	23
5.4 Effect of the Bottom Plate Anchorage Methods.....	25
5.5 Uplift Displacement of the End Stud.....	27
5.6 Ductility.....	28
5.7 Modeling of Shear Walls without Perforations.....	28
5.8 Modeling of Perforated Shear Walls.....	31
6. Summary and Conclusions.....	36
7. Recommendations for Future Research.....	37
8. References.....	38
Appendix A. Bottom Plate Nail Withdrawal Tests	
Appendix B. Analysis of the Failure Modes of the Shear Wall Bottom Plate	
Appendix C. Metric Conversion Factors	

List of Tables

Table 1. Comparison of Analytical Models	9
Table 2. Wall Configurations.....	10
Table 3. Wall Materials and Construction Data.....	11
Table 4. Fastening Schedule	12
Table 5. Performance Parameters of Bolted Shear Walls	20
Table 6. Performance Parameters of Nailed Shear Walls	21
Table 7. Failure Modes (Bolted Walls).....	22
Table 8. Summary of Anchor Bolt Loads	26
Table 9. Comparison of Analytical and Experimental Results	30
Table 10. Unit Shear Values	32
Table 11. Comparison of Experimental and Estimated (PSW method) Shear Wall Capacity	33
Table 12. Comparison of Experimental and Estimated (PSW method) Shear Wall Stiffnesses	34
Table 13. Comparison of Experimental and Estimated (Forintek method) Shear Wall Capacity	36

List of Figures

Figure 1. Corner Construction for Bolted Walls.....	13
Figure 2. Wall Setup and Instrumentation.....	14
Figure 3. Wall Test Setup	15
Figure 4. Load - Deflection Relationships for Bolted Walls without Perforations	17
Figure 5. Load - Deflection Relationships for Bolted Walls with Perforations	18
Figure 6. Load - Deflection Relationships for Nailed Walls without Perforations	18
Figure 7. Load - Deflection Relationships for Nailed Walls with Perforations	19
Figure 8. Rigid Body Rotation of the Loaded End of Nailed Walls	23
Figure 9. Corner Return Failure (Wall 6)	24
Figure 10. Response of Sheathing Nails along the Bottom Plate of a Corner	24
Figure 11. Wall Uplift Displacement vs. Wall Deflection (Bolted Walls).....	27
Figure 12. Wall Uplift Displacement vs. Wall Deflection (Nailed Walls).....	28
Figure 13. Comparison of Experimental Data for Walls without Perforations with the Analytical Models	31
Figure 14. Effect of Components above and below Windows	32
Figure 15. Comparison of Experimental and Predicted (PSW Method) Shear Wall Capacity (Bolted Walls)	33
Figure 16. Comparison of Experimental and Predicted (PSW Method) Shear Wall Capacity (Nailed Walls)	34
Figure 17. Comparison of Experimental and Predicted (PSW Method) Shear Wall Stiffness at 0.1 Inch Deflection (Bolted Walls)	35
Figure 18. Comparison of Experimental and Predicted (PSW Method) Shear Wall Stiffness at 0.1 Inch Deflection (Nailed Walls)	35

1. Introduction

Although the majority of residential structures in the United States are built using conventional construction practices, current U.S. building codes fail to provide methods for structural analysis of the lateral force resisting system of traditional light-frame buildings. Instead, the building codes specify prescriptive provisions that are believed to meet or exceed the strength and serviceability criteria, but provide the designer with little guidance for understanding the performance of the structure. Development of simplified analytical methods that accurately model the response of conventional construction will promote efficient design and more clearly define performance criteria for alternative methods of residential construction.

Shear walls are the primary part of the lateral force resisting system for light-frame buildings. Sheathing-to-frame connections, anchorage methods, aspect ratio of braced wall panels and braced wall line, and type and size of perforations are the major factors that govern the response of light-frame wood shear walls. Sheathing connections resist shear forces, whereas anchors resist uplift forces. The choice of the anchorage method affects the shear wall stiffness, capacity, and failure mode. The latter can further influence ductility and seismic resistance of the shear wall.

Because many traditional design methods are unsuccessful in predicting the realistic lateral response of conventional wood shear walls, there is a difference of opinion regarding the actual wind and seismic resistance of light-frame buildings. One factor contributing to this controversy is the effect of the complete building assembly on the response of an individual shear wall. Realization of this system effect will improve the understanding of conventional wood shear walls and facilitate the development of analytical methodologies for their design.

This study was designed to provide empirical and analytical insights into the response of shear walls with corner framing and to determine the uplift load sharing mechanism between the adjacent walls. The project objectives included:

- (1) measuring the performance of conventional wood shear walls (i.e., no hold-downs) and comparing results with the data for engineered wood shear walls (i.e., including hold-downs);
- (2) investigating the restraining effect of the corner return on the lateral response of conventional wood shear walls; and,
- (3) examining the applicability of innovative design methods to conventional wood shear walls restrained against overturning by corner framing.

2. Scope and Limitations

The findings of this study are generally limited to the conditions investigated herein. The effects of other wall geometries, sheathing fastener sizes, types of panels including interior sheathing panels, gravity load, and loading at an oblique angle to the shear wall plane are the kind of factors that should be considered when interpreting the findings of this report. However, the results of this project demonstrate a general trend in the response of conventional wood shear walls and are a valuable source of information for understanding the performance and design of conventional wood frame buildings.

3. Background

A voluminous body of experimental and analytical data can be found in the literature on the performance of light-frame wood shear walls. However, most of the experimental work in the United States was done according to the ASTM Standard E 72 - 95 “Standard Test Methods of Conducting Strength Test of Panels for Building Construction” or ASTM Standard E 564 - 95 “Standard Practice for Static Load Tests for Shear Resistance of Framed Walls for Buildings”[1]. Both standards require full anchorage of the wall to the foundation so that it can develop its maximum shear resistance. This practice misrepresents the response of conventional shear walls which are typically built without metal hardware at the corners and around openings. Moreover, the majority of the tests were conducted for two-dimensional shear wall assemblies that neglected three-dimensional force distribution. Similarly, most of the design methods found in the literature were formulated for the walls fully restrained against overturning. Only recently, new studies undertaken at Forintek Canada Corp., Canada [2][3], Virginia Tech, Blacksburg, VA, USA [4][5][6][7], and NAHB Research Center, Upper Marlboro, MD, USA [8][9] provided empirical data and analytical methodologies towards modeling the behavior of conventional wood shear walls. A summary of the relevant research conducted in the field of light-frame wood shear walls follows.

Sugiyama and Yasumura [10] conducted tests studying one-third scale monotonic racking tests of wood stud, plywood sheathed shear walls with openings. The loads required to displace the wall at a shear deformation angle of 1/60, 1/75, 1/100, 1/150, and 1/300 were monitored. The researchers defined the sheathing area ratio, r , to classify walls based on the amount of openings and to investigate empirical relationships to strength and stiffness (Equation (1)).

$$r = \frac{1}{1 + \frac{A_o}{H \sum L_i}} \quad (1)$$

where:

- A_o = total area of openings;
- H = height of the wall; and,
- $\sum L_i$ = summation of length of all full height wall segments.

Sugiyama and Matsumoto [11] determined an empirical equation to relate shear capacity and sheathing area ratio, based on the scaled tests. According to Sugiyama and Matsumoto the empirical equation (Equation (2)) relates the ratio, F , of the shear load for a wall with openings to the shear load of a fully sheathed wall at shear deformation angle of 1/100 radians and for ultimate capacity. This method was referred to as the perforated shear wall (PSW) method.

$$F = \frac{r}{3 - 2r} \quad (2)$$

Dolan and Johnson [12] conducted an experimental study on the performance of perforated wood shear walls with varying sheathing area ratios. The objective of the research was two-fold. The first objective was to verify the work of Sugiyama using full scale tests, and the second objective was to determine a relationship between the ultimate capacity of a shear wall when tested monotonically versus the ultimate capacity of the same wall configuration tested under cyclic loading. Ten 8 x 40 foot¹ walls were tested. Five different sheathing area ratios were used, with each wall type tested once monotonically and once cyclically. The wall framing consisted of No. 2 grade Spruce-Pine-Fir (SPF) studs spaced 16 inches on center. Exterior sheathing was 15/32-

¹ See Appendix C for metric conversion factors.

inch-thick plywood and the interior sheathing was 1/2-inch-thick gypsum wallboard (GWB). Two hold-down anchors, one located at each end of the 40 foot wall specimen, were installed to provide the end restraint as required by the PSW method. The predicted load capacities calculated using Equation (2) were in good agreement with the experimental results (conservative by approximately 10 percent). All drywall tape joints around openings cracked and some tape joints between fully sheathed panels failed as expected during the loading. The shear capacity was governed by the connection of the structural sheathing to the framing which was the desired behavior. Hold-down anchors experienced no failure during the tests. In summary, the full scale tests confirmed the previous model scale tests by Sugiyama, and thus validated the PSW method.

Dolan and Heine [4] extended the research on the behavior of the perforated shear walls. There were two objectives of this study. The first was to quantify the effects of overturning restraint on full scale wood frame shear walls, with and without openings, tested monotonically. The second objective was to determine the applicability of the PSW method to conventionally built walls without considering overturning restraint provided by the hold-down devices.

Six 8 x 40 foot walls were tested. Three different sheathing area ratios were used with each wall type tested monotonically, once with no hold-down devices and once with the maximum number of hold-downs (one at the each end of the specimen and on both sides of all openings). The wall framing consisted of No. 2 grade SPF studs spaced 16 inches on center. Exterior sheathing was 7/16-inch-thick oriented strand board (OSB) and the interior sheathing was 1/2-inch-thick GWB. Together with the results from Dolan and Johnson [12] three different wall configurations with three different end restraints were tested.

Shear walls designed according to the PSW method as opposed to traditional design had a lower ultimate capacity and stiffness as expected. This difference was roughly 10 percent and is addressed in the PSW equations. Ultimate capacity and stiffness were further reduced when hold-down anchors were completely omitted. The data suggested that the PSW approach produced conservative design values for walls constructed according to the method (i.e. hold-down restraints provided only at the ends of the wall line).

Dolan and Heine [5] investigated the effects of overturning restraint on full-scale wood frame shear walls, with and without openings, tested cyclically using the Sequential Phased Displacement (SPD) protocol [13].

Six 8 x 40 foot walls were tested. Three different sheathing area ratios were used with each wall type tested cyclically, once with no hold-down devices and once with the maximum number of hold-downs (one at the each end of the specimen and on both sides of all openings). The wall framing consisted of No. 2 grade SPF studs spaced 16 inches on center. Exterior sheathing was 7/16-inch-thick OSB and the interior sheathing was 1/2-inch-thick GWB. Together with the results from Dolan and Johnson [12] three different wall configurations with three different end restraints were examined. The ultimate capacity of the walls subjected to SPD loading increased with increasing overturning restraint, as with the monotonic tests. The ultimate capacity reached during the SPD tests was essentially identical to that achieved in the monotonic tests based on the initial “envelope” of the hysteresis curves.

Dolan and Heine [6] studied the effects of corners on uplift restraint of wood frame shear walls tested cyclically using the SPD protocol. Four walls, 12 feet in length and 8 feet in height were tested. Attached to the ends were 4 x 8 foot or 2 x 8 foot corner segments. Each wall configuration was tested twice. Each specimen was constructed using identical framing, sheathing, nails, and nailing schedule. The wall framing consisted of No. 2 SPF studs spaced 16 inches on center. Exterior sheathing was 7/16-inch-thick OSB and the interior sheathing was 1/2-inch-thick GWB.

Corner framing generally provided a hold-down effect that increased wall capacity when compared with walls without overturning restraints. On average, walls with 4-foot corner returns reached slightly higher ultimate capacities than specimens with 2-foot corner returns. The 2-foot and 4-foot corner returns provided sufficient end restraint to develop 85 percent and 90 percent, respectively, of the shear resistance of the fully-restrained walls. Improvements in ductility were also observed.

In all of the previously discussed studies, the base anchorage of the bottom plate was provided by 5/8 inch diameter anchor bolts with 3 x 3 x 1/4 inch plate washers and hold-downs (or no hold-downs) as described in [4], [5], [6], and [12].

The objective of the research conducted by the NAHB Research Center [8] was to confirm the use of the PSW method and to determine the performance of full-scale shear walls with 2-foot wall segments (4:1 aspect ratio), reduced base restraint, and the use of alternative framing practices. A total of seven 8 x 16 or 20 foot shear wall specimens were tested in this investigation. The wall framing consisted of SPF Stud grade lumber. Exterior sheathing was 7/16-inch-thick OSB and the interior sheathing was 1/2-inch-thick GWB. Pneumatic fasteners were used throughout the testing program. Hold-downs were installed at the ends of the wall specimens in accordance with the PSW method.

Two specimens in this research program were constructed using alternative framing practices. A garage opening specimen was constructed using one 1,000 pound capacity strap on each end of the specimen. The continuous strap was connected to the exterior sheathing side of the jack stud assembly, wrapped over the header/double top plate, and connected to the interior sheathing side of the jack stud assembly. The second alternative framing method introduced the use of truss plates to reinforce framing joints at wall corners and opening corners that were considered to be “weak links” in previous testing. The truss plates were installed on each side of the framing using a mallet. The truss plates were 3 x 6 inches with 144 teeth (0.4 inches long) per truss plate. Because the truss plates created an integral hold-down with the framing and anchor bolt at the end of the wall, no hold-downs were installed on this specimen.

The shear capacity calculated using Equation (2) conservatively estimated the capacity of all specimens. The use of an alternative empirical equation (Equation (3)) resulted in a more accurate prediction of capacity on average.

$$F = \frac{r}{2 - r} \quad (3)$$

where:

F and r = see Equations (1) and (2).

In addition, increasing anchor bolt spacing from 2 feet to 6 feet only slightly decreased the ultimate capacity, initial stiffness, and dissipated energy. Equation (2) conservatively estimated the capacity of walls with increased anchor bolt spacing. The alternative framing practices

investigated in this report showed promise for high-wind and high-seismic applications with the optional enhancements of the PSW method.

Another study was undertaken by the NAHB Research Center [9] with the objective to provide additional information about the performance of full-scale tests with 2-foot wall segments and various conventional and innovative methods of providing base restraint. This research expanded the scope of the PSW method. A total of eight 8 x 20 foot shear wall specimens were tested in this investigation. The wall framing consisted of SPF Stud grade lumber. Exterior sheathing was 7/16-inch-thick OSB and the interior sheathing was 1/2-inch-thick GWB. Pneumatic fasteners were used throughout the testing program.

Hold-downs were installed at the ends of the wall specimens in accordance with the PSW method. In addition to the hold-downs, the bottom plate of the specimens were anchored with either 5/8-inch diameter bolts at 2 foot on center, 5/8-inch diameter bolts 6 foot on center, or two 16d pneumatic nails 3 inches in length and 0.131 inches in diameter at 16 inches on center. An alternative framing practice in one specimen utilized an 18 gauge (0.043 inch thick) galvanized steel strap to attach each stud to a wood beam using four 10d bright common nails on each side of the strap.

The data presented additional verification of the PSW method using reduced base restraint and 2-foot wall segments. The wall capacity calculated using Equation (2) conservatively estimated the shear capacity of all specimens. The use of the alternative empirical equation (Equation (3)) resulted in a more accurate prediction of ultimate capacity. This research produced similar results to the previous test with regard to increasing anchor bolt spacing [8]. The use of a 6 foot on center anchor bolt spacing slightly decreases the ultimate capacity, initial stiffness, and dissipated energy. Similar reductions were observed with the use of nailed sole plate anchorage in comparison to anchor bolts at 2 feet on center. However, in general, walls with nailed sole plates performed better than walls with anchor bolts 6 feet on center. Despite these decreases Equation (2) conservatively estimated the capacity with either increased anchor bolt spacing or sole plate nails, even when using a fully sheathed wall with anchor bolts at 2 feet on center as the reference. The amount of shear resistance (base anchorage) needed at the sole plate can be reasonably determined using Equation (2) or (3) with perforated shear walls. The alternative framing practice investigated in this report displayed promise as a simple and strong solution for high-wind and high-seismic applications.

Thurston [14] reported results of an experimental study of the performance of light-frame shear walls with low aspect ratios (1.875:1 or less), various openings, and sheathing types. The author indicated that the resistance of a conventional shear wall tested as an individual component could be significantly underestimated due to neglecting the system effects present in a three-dimensional building assembly. Based on an extensive literature survey, the author concluded that the lateral force resisting system of conventionally constructed houses showed adequate performance under the in-service loads. The testing program included shear walls assembled without hold-down devices. Instead, the overturning moment was resisted with 4-foot corner returns. The bottom plate was nailed to the wood foundation with pairs of 0.157 inch diameter and 3.9 inch long nails spaced at 23.6 inches on center. The sheathing panels were nailed to the framing with 0.098 inch diameter nails. The walls were tested using a quasi-static reverse cyclic loading protocol. Using results of the study, the author demonstrated that the hold-down devices were unnecessary around the window openings because the components under the windows

prevented rotation of the adjacent braced wall panels. However, the walls with door openings required additional strapping to prevent premature wall degradation due to overturning of the segments adjacent the door openings.

Ni et al. [3] introduced a design method for analysis of perforated shear walls with various overturning restraints and gravity loads. The model was formulated based on the assumption that the total resistance of a perforated shear wall was defined by the sum of the resistances of the full-height wall segments and wall components above and below openings (Equation (4)).

$$V = \sum_{i=1}^n J_{hd}^i v_d^i L_s^i + \sum_{j=1}^m J_c^j v_d^j L_c^j \quad (4)$$

where:

- V = lateral load capacity of shear wall;
- J_{hd} = hold-down modification factor;
- v_d = unit shear capacity based on full overturning restraint;
- L_s = length of full-height shear wall segment;
- J_c = modification factor for wall components above or below opening;
- L_c = length of wall component above or below opening;
- n = number of full-height segments; and,
- m = number of wall components.

The hold-down modification factor, J_{hd} , was derived based on experimental data (Equation (5)). This factor was a strength reduction coefficient that was equal to unity for fully restrained walls or had a value between zero and unity for walls with intermediate restraint conditions.

$$J_{hd} = \frac{1}{1 + \frac{H}{L_s} \left(1 - \frac{P_u}{v_d H}\right)^3} \quad (5)$$

$$0 \leq \frac{P_u}{v_d H} \leq 1 \quad (6)$$

where:

- H = shear wall height; and
- P_u = uplift resistance of a shear wall segment due to hold-down, vertical load, and adjacent wall components.

The modification factor, J_c , for the wall components below openings was assumed to be unity, whereas J_c for the wall components above openings was calculated with Equation (7).

$$J_c = \frac{1}{1 + \frac{L_c}{H_c}} \quad (7)$$

To facilitate the use of the presented method, the authors simplified the formulation of the model by ignoring the contribution of the wall components above and below openings and using the hold-down modification factor of unity ($J_{hd} = 1$) for the shear wall segments restrained against uplift at the ends or computed with Equation (8) for the segments without restraints.

$$J_{hd} = \frac{1}{1 + \frac{H}{L_s}} \quad (8)$$

The authors validated both models and compared tests results with the PSW method. The first method (Equations (4), (5), and (7)) showed good agreement with experimental data; the simplified method (Equations (4) and (8)) provided more conservative results.

Ni and Karacabeyli [2] studied the effect of overturning restraints on the performance of conventional and engineered shear walls without perforations. The researchers developed a mechanics-based model that estimated capacity of shear walls with various overturning restraints including hold-down brackets, gravity loads, and perpendicular walls. The model (Equation (9)) was formulated using the principle of equilibrium of the shear and uplift forces.

$$\alpha = \sqrt{1 + 2\phi\gamma + \gamma^2} - \gamma \quad (9)$$

$$\phi = \frac{P}{M C_N}, \quad 0 \leq \phi \leq 1 \quad (10)$$

where:

- α = ratio of the lateral load capacity of wall with partial uplift restraint to capacity of wall with full uplift restraint;
- γ = wall aspect ratio;
- ϕ = uplift restraint effect which is equal to unity for the wall fully restrained against uplift;
- M = total number of nails along the end stud of a shear wall segment;
- C_N = capacity of a single nail connection; and,
- P = uplift restraint force on the end stud of shear wall.

The model was validated using results from a testing program on shear walls with different aspect ratios and restraint effects under cyclic and monotonic loading. Although the model provided conservative predictions, the results were consistent with the trend found from the experimental data. The researches also developed an empirical method for estimating the shear capacity for walls without overturning restraints (Equation (11)) and with intermediate overturning restraints (Equation (12)). The models were formulated based on the assumption of an inverse relationship between unit shear capacity and wall aspect ratio.

$$\alpha = \frac{1}{1 + \gamma} \quad [\text{no restraint}] \quad \phi = 0 \quad (11)$$

$$\alpha = \frac{1}{1 + \gamma(1 - \phi)^n} \quad [\text{partial restraint}] \quad 0 \leq \phi \leq 1 \quad (12)$$

where:

- α, γ, ϕ = see Equation (9); and
- $n = 3$ = nonlinear parameter found through statistical fit of the model to the test data.

Note that Equation (11) is equivalent to Equation (8) and Equation (12) is equivalent to Equation (5). Predictions of the empirical model followed the experimental results more closely as compared to the mechanics-based model. Analysis of the test results showed that the wall stiffness within the range of linear behavior was similar for the engineered and conventional shear walls, whereas the displacement at peak load was larger for the engineered walls. A vertical load of 1.2 kip/ft on unrestrained walls was required to provide the same performance as the wall with hold-downs. However, vertical load of 0.3 kip/ft, which counteracted 25% of the overturning moment, allowed the unrestrained wall to develop 80% of its full capacity and ultimate displacement. The last conclusions were validated for shear walls with aspect ratio $\gamma = 1$.

Salenikovich and Dolan [15] investigated the performance of fully sheathed light-frame wood shear wall segments with conventional and engineered overturning restraints. The study ignored the effect of gravity load and corner framing on uplift resistance of walls with conventional restraints. Walls with aspect ratios of 4:1, 2:1, 1:1, and 2:3 were tested using monotonic and reversed cyclic loading protocols. Results of the study showed that the unit shear of the engineered shear walls was independent of the wall aspect ratio, whereas a strong inverse trend was found between the aspect ratio and the unit shear for walls without hold-downs. Conventional walls with high aspect ratios exhibited higher ductility as opposed to the walls with low aspect ratios. The rigid body rotation prevailed in the response of conventional shear walls resulting in the premature failure due to separation of the panels along the bottom plate. The researchers also investigated the effect of the decreased sheathing nail edge distance along the top and bottom plates on the shear wall performance. The walls with decreased edge distance exhibited a 20% reduction in capacity and a 30% reduction in deflection at failure.

Salenikovich [7] developed a mechanics-based model (Equation (13)) that predicted the capacity of light-frame wood shear walls without overturning restraints from hold-downs, dead load, or corners. The model was derived based on the principle of static equilibrium of the forces present in the panel-frame assembly. A uniform nail force distribution along the bottom plate was assumed for both horizontal and vertical directions.

$$r = \frac{1}{\sqrt{1 + \left(\frac{2\alpha}{n}\right)^2}} \quad (13)$$

where:

- α = aspect ratio of a single panel in the wall;
- n = number of panels in the wall; and,
- r = ratio of the lateral load capacity of wall without uplift restraint to capacity with full uplift restraint.

The model showed excellent agreement with the experimental results for shear walls with up to four panels. However, because of the assumption of the uniform force distribution along the bottom plate, the accuracy of the model decreased as the number of panels in the wall increased. The analysis also showed that the adjacent panels provided uplift restraint for each other, resulting in higher unit shear resistance for shear walls with several panels in the assembly as compared to a single panel shear wall.

As compared to the model proposed by Ni and Karacabeyli [2], the model developed by Salenikovich [7] provided less conservative results (Table 1). The comparison assumed no uplift

restraint ($\phi = 0$, see Equation (10)). Neither of these two models addressed the behavior of perforated shear walls.

TABLE 1
COMPARISON OF ANALYTICAL MODELS

Wall Aspect Ratio	Shear Strength Reduction Factor	
	Ni and Karacabeyli [2], $j = 0$	Salenikovich [7]
2	0.24	0.24
1	0.41	0.45
0.66	0.54	0.60
0.5	0.62	0.71

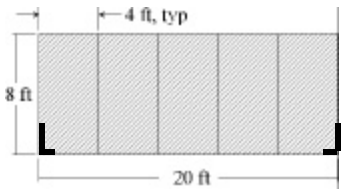
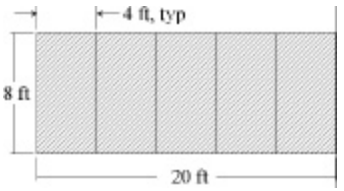
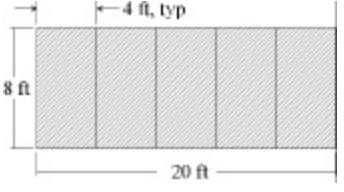
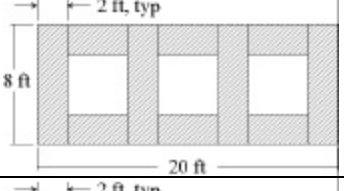
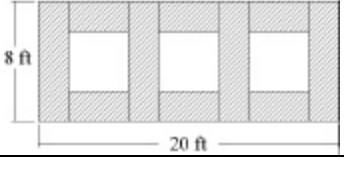
In light of the above discussion, the models developed by Ni et al. [3] and Ni and Karacabeyli [2] are the most appropriate for the analysis of conventional wood shear walls because they provide methods to include the overturning resistance from gravity load and corner framing. Therefore, these models predict shear wall response in a manner that is more representative of walls within the boundary conditions imposed by the building. The models also provide the engineer with a sense of the mechanics involved in the force distribution in a shear wall assembly.

4. Experimental Program

4.1 Wall Construction

Eleven 8 x 20 foot wood shear walls framed using conventional construction practices were tested. Table 2 summarizes the wall configurations. Tables 3 and 4 summarize the wall materials, construction data, and fastening schedule. Two wall base restraints were investigated: (i) bottom plate bolted to the foundation with 5/8-inch anchor bolts spaced 6 feet on center, and (ii) bottom plate nailed to a wood platform with four 16d pneumatic nails (3-1/4 inch long x 0.131 inch diameter) every 16 inches at wall braced panels and two nails every 16 inches under openings. Hereinafter the first wall construction type is referred to as bolted wall and the second as nailed wall.

TABLE 2
WALL CONFIGURATIONS

Wall #	Wall Configuration	Openings	r	Bottom Plate Connection	Anchorage Method
Wall 1		None	1.0	5/8 inch bolts 6 feet on center	Hold-down anchors on both ends
Wall 2		None	1.0	5/8 inch bolts 6 feet on center	2 ft corner return with 1 bolt
Wall 3		None	1.0	5/8 inch bolts 6 feet on center	4 ft corner return with 2 bolts
Wall 4		Three 4ft x 4ft	0.57	5/8 inch Bolts 6 feet on center	2 ft corner return with 1 bolt
Wall 5		Three 4ft x 4ft	0.57	5/8 inch Bolts 6 feet on center	4 ft corner return with 2 bolts

**TABLE 2
WALL CONFIGURATIONS
(continued)**

Wall #	Wall Configuration	Openings	r	Bottom Plate Connection	Anchorage Method
Wall 6		Two 4 ft x 4 ft	0.75	5/8 inch Bolts 6 feet on center	4 ft corner return with 2 bolts
Wall 7		None	1.0	16d pneumatic nails	2 ft corner return with 6 nails
Wall 8		None	1.0	16d pneumatic nails	4 ft corner return with 12 nails
Wall 9		Three 4 ft x 4 ft	0.57	16d pneumatic nails	2 ft corner return with 6 nails
Wall 10		Three 4 ft x 4 ft	0.57	16d pneumatic nails	4 ft corner return with 12 nails
Wall 11		Two 4 ft x 4 ft	0.75	16d pneumatic nails	4 ft corner return with 12 nails

**TABLE 3
WALL MATERIALS AND CONSTRUCTION DATA**

Component	Construction and Materials
Hold-down (Wall 1 only)	Simpson HTT 22 [18], nailed to end studs with 32-16d sinker nails (3-1/4 inch long x 0.148 inch diameter)
Anchor bolts	5/8 inch diameter bolts with 1-5/8 inch diameter cut washer
Framing members	2 x 4 SPF lumber
Framing nails ¹	16d short full-round-head bright basic pneumatic nails (3-1/4 inch long x 0.131 inch diameter)
Exterior sheathing	7/16-inch-thick OSB panel (APA rated 24/16)
Sheathing Nails ¹	8d full-round-head bright basic pneumatic nails (2-3/8 inch long x 0.113 inch diameter)
Interior Sheathing	None

¹Nails were manufactured by Senco Products, Inc., Cincinnati, Ohio.

**TABLE 4
FASTENING SCHEDULE**

Connection	Fastener	Spacing
Top plate to top plate (face-nailed)	16d pneumatic	12 inches on center
Top plate to top plate lap connection at the corner	3-16d pneumatic	per connection
Top/bottom plate to stud (end-nailed)	2-16d pneumatic	per connection
Stud to stud (face-nailed)	2-16d pneumatic	24 inches on center
Stud to window sill plate and header (end-nailed)	2-16d pneumatic	per stud
Hold-down (Wall 1 only)	32-16d sinker	per hold-down
Bottom plate to platform at braced wall panels (Walls 7-11)	4-16d pneumatic ¹	16 inches on center
Bottom plate to platform under openings (Walls 7-11)	2-16d pneumatic ¹	16 inches on center
Bottom plate to platform (Walls 1-6)	anchor bolts	6 feet on center
Corner return to wall end stud ²	16d pneumatic	24 inches on center
Sheathing panels to framing	8d pneumatic	6 inches on perimeter 12 inches in field

¹Approximately 50 percent of nails penetrated the subfloor panel and the rim joist, and 50 percent only the subfloor panel.

² Sheathing panels at the corner were also connected to the end stud.

The anchor spacing of the bolted walls was consistent with the provisions of Section R403.1.6 of "International Residential Code for One- and Two-Family Dwellings" [16]. The first and last anchor bolts were located at twelve inches from the corner of the wall. The nailing schedule for the nailed walls was in compliance with the requirements of NER-272 "Power Driven Staples, Nails, and Allied Fasteners for Use in All Types of Buildings Construction" [17]. The nails were staggered so that every other nail penetrated the 23/32-inch-thick OSB subfloor panel (APA rated 24 inches on center) and the SPF rim joist, whereas the rest of the nails penetrated only the OSB subfloor panel. Appendix A reports the results of the individual nail withdrawal tests.

With the exception of Wall 1 which was secured to the foundation with hold-downs, a corner return was framed at the loaded end of each wall to provide overturning restraint. The other wall attributes were kept the same throughout the testing program. Wall 1 was tested to define a comparative performance case using the response of the wall restrained against overturning with hold-downs. Throughout this document this wall construction is referred to as engineered.

To investigate the effect of the corner return width on overturning resistance, the walls were tested with 2-foot and 4-foot wide corners. The former was framed with studs spaced 24 inches on center, and the latter with studs spaced 16 inches on center. For bolted walls, the 2-foot corners were secured to the platform with one anchor bolt positioned at 12 inches from the corner, and the 4-foot corners were attached with two bolts spaced 24 inches on center. For nailed walls, the 2-foot corners were attached with six nails and the 4-foot corners with twelve nails. The nails were spaced and staggered as specified in Table 4. Figure 1 depicts the corner construction for the bolted walls. Except for the bottom plate attachment, the same corner construction was used for the nailed walls.

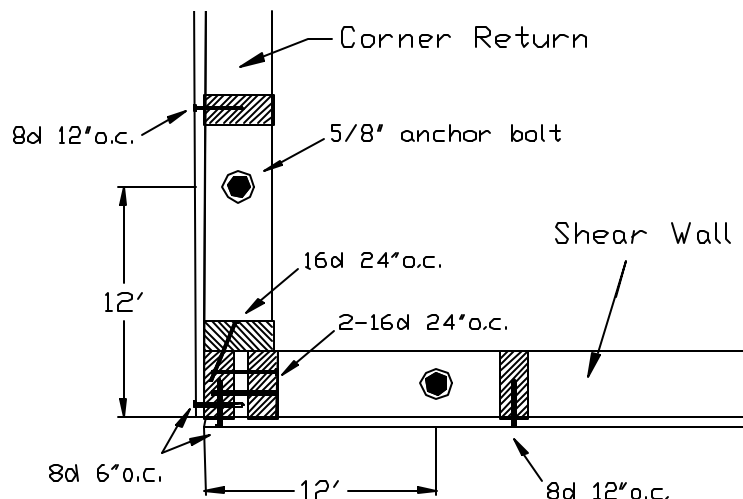


FIGURE 1
CORNER CONSTRUCTION FOR BOLTED WALLS

To investigate the effect of perforations on the performance of conventionally constructed walls, six specimens were framed with 4 x 4 foot window-type openings. Sheathing area ratios, r (Equation (1)), of 0.57 and 0.75 were used. The sheathing panels were attached so that the full height segments did not extend into the areas above and below openings. Therefore, there was no direct shear transfer through the braced wall panels into the sheathed wall components above and below openings.

The walls were constructed with 2 x 4 inch nominal SPF Stud grade lumber. The top and bottom plates were framed with 2 x 4 x 120 inch nominal SPF No. 2 grade lumber. The double top plate was also framed with 2 x 4 x 96 inch nominal SPF Stud grade lumber to provide a 2-foot splice joint offset. Studs were spaced at 16 inches on center. Stud spacing was increased to 24 inches on center for Walls 4, 5, 9, and 10 to coincide with the investigation of 2-foot wall segments. The walls were sheathed with 7/16-inch-thick OSB panels (APA rated 24/16). The OSB panels were oriented in the vertical direction and were attached to the framing using 8d full-round-head bright basic pneumatic nails (2-3/8 inch long x 0.113 inch diameter) spaced 6 inches along the perimeter and 12 inches in the field of the panels. A nail edge distance of 3/4 inch along the top and bottom plates was maintained. The wall frame was assembled with 16d short full-round-head bright basic pneumatic nails (3-1/4 inch long x 0.131 inch diameter). All nails were installed using a Senco® SN65 pneumatic nail gun.

The tests were conducted in an indoor shear wall testing facility located at the NAHB Research Center, Inc., Upper Marlboro, MD. The walls were constructed one at a time and typically tested within two days after the fabrication. Nailed walls were tested at least 24 hours after nailing of the bottom plate to the platform to allow for partial stress relaxation in the connections. After each test, the moisture content of the frame members was determined using an electric moisture meter according to Method A (Conductance Meters) of ASTM Standard D 4444-92 [19]. Specific gravity of the selected frame members was determined using small samples according to Method B (Volume by Water Immersion) of ASTM Standard D 2395-93 [19].

4.2 Test Procedure and Wall Instrumentation

Figures 2 and 3 show the shear wall test setup and instrumentation. The walls were tested in a vertical position. The top plate was attached to the distribution beam with 1/2-inch diameter bolts spaced 24 inches on center. One-directional load was applied to the shear wall by displacing the distribution beam with a 100,000 lb capacity hydraulic actuator with an eight inch travel range at a constant rate of 0.3 inch/min. The distribution beam was braced with two sets of rollers that restricted the wall displacement outside the plane of loading and allowed the beam to move with minimum friction resistance. The walls were displaced by a minimum of 5.0 inches or until wall failure, whichever occurred first. Load was measured with a 100,000 lb capacity electronic load cell located between the distribution beam and the hydraulic actuator. Because the hydraulic actuator was attached between the steel frame and test wall using pinned connections, uplift of the wall caused rotation of the cylinder that produced an increasing uplift force component acting on the wall. This additional force had a conservative effect on the response of walls restrained with corners. A 2 x 4 inch nominal wood spacer was used between the distribution beam and the wall to allow for rotation of the sheathing panels without interfering with the distribution beam.

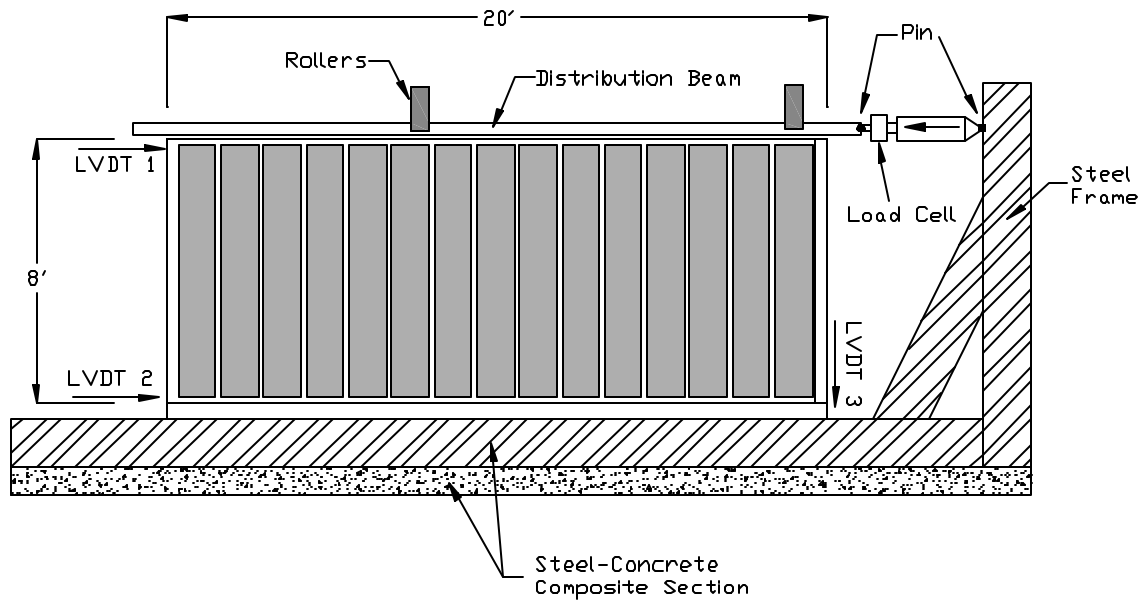


FIGURE 2
WALL SETUP AND INSTRUMENTATION

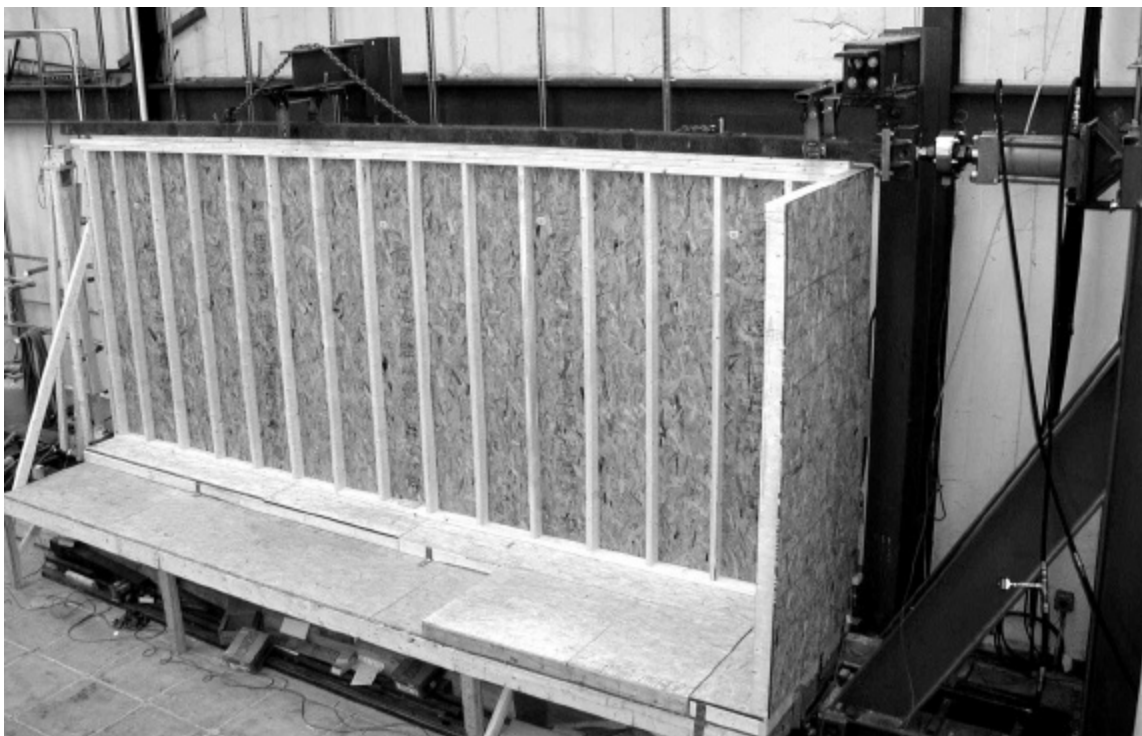


FIGURE 3
WALL TEST SETUP

Deformations of the wall were measured with a set of three linear variable differential transformers (LVDT). Displacements of the top and bottom plates were measured relative to the platform with LVDT 1 and LVDT 2, respectively (Figure 2). Displacement of the bottom plate was subtracted from displacement of the top plate to compute the story drift. This adjusted data was used to plot the load-displacement curves. Uplift displacement of the end stud was measured relative to the platform with LVDT 3. To enable direct comparison of the uplift data between Wall 1 (without corner) and the walls with corners, the OSB panels on the corner were drilled to allow attachment of LVDT 3 to the end stud preventing the corner panel slip from affecting the uplift readings. The drilled holes did not interfere with the nailing schedule. The same distance between the core of LVDT 3 and the end stud was maintained for all tests.

Ring-shaped electronic load cells were used to measure the uplift forces resisted by the anchor bolts in the vicinity of the loaded end of the wall and the corner (Figure 9). These load cells were set onto the bottom plate through the anchor bolts. A 1-5/8 inch diameter washer was placed between the bottom plate and the load cell. The bolts were then tightened directly onto the load cell. The hold-down anchor bolt (Wall 1) was tightened to a value of 2,000 lb and the remaining anchors were tightened to a value of 300 lb. This was done to ensure consistency throughout the testing program. The force resisted by the hold-down anchor bolt was measured by a load cell placed under the test platform. Because the tension force was partially counteracted by the friction force between the bolt and the platform, the measurements underestimated the actual tension force resisted by the hold-down. Monitoring of the bolt forces above and below the platform for another wall showed that friction could decrease the measured uplift force by as much as 500 lb.

A computer-based data acquisition system [20] was used to record the data at a sampling rate of 1 Hz.

4.3 Definition of the Shear Wall Performance Parameters

Wall capacity, P_{max} , was defined as the maximum load from the load-displacement curve. Failure load was defined as the point on the load-displacement curve where the load degraded to 80 percent of the wall capacity. Other parameters were determined based on the equivalent energy elastic-plastic (EEEP) response curve [13]. The proportional limit was defined at a load equal to 40 percent of the wall capacity. Yield load was determined from the EEEP response curve by equalizing the energy dissipated by the wall until failure with the energy of the ideal elastic-plastic model. In the cases when the wall did not fail, the displacement at the last point on the curve was used as the displacement at failure load. Elastic stiffness was determined as the slope of a straight line passing through the initial point and the proportional limit. In addition, stiffness at a deformation of 0.1 inch was computed by statistical fitting of a straight line in the data range between 0.0 and 0.1 inch wall deflection. The former stiffness parameter is a function of the wall capacity, whereas the latter is a displacement-based property independent of the post-linear response.

The inelastic performance of the walls was assessed using ductility ratios and a toughness of failure index. These parameters index a wall's relative ability to undergo deformations while resisting high loads. Two ductility ratios were calculated (Equations (14) and (15)). The first was based on the peak displacement, whereas the second was based on the failure displacement.

$$\text{ductility ratio 1} = \frac{\Delta_{\text{peak}}}{\Delta_{\text{yield}}} \quad (14)$$

$$\text{ductility ratio 2} = \frac{\Delta_{\text{failure}}}{\Delta_{\text{yield}}} \quad (15)$$

where:

Δ_{peak} = displacement at maximum load;

Δ_{yield} = displacement at yield load; and,

Δ_{failure} = displacement at failure load.

The toughness of failure index was computed using Equation (16).

$$\text{toughness of failure index} = \frac{\Delta_{\text{failure}}}{\Delta_{\text{peak}}} \quad (16)$$

5. Results and Discussion

5.1 General

Figures 4 and 5 display load-displacement curves for the bolted walls without and with perforations, respectively. Figures 6 and 7 display load-displacement curves for the nailed walls without and with perforations, respectively. Tables 5 and 6 summarize the shear wall performance parameters for the bolted and nailed walls, respectively. A detailed analysis of the experimental results is given in the following sections. However, the load-displacement curves indicate the major trends in the performance of the shear walls. The 4-foot corners increase the wall strength, ductility, and work until failure as compared to the 2-foot corners with the improvements more evident for the walls without perforations. The elastic stiffness is governed by the sheathing area ratio and is essentially unaffected by the corner width. The overturning resistance provided by the corners is more effective for the perforated walls than for the walls without perforations. The type of the bottom plate anchorage (bolts vs. nails) has a marginal influence on the wall response.

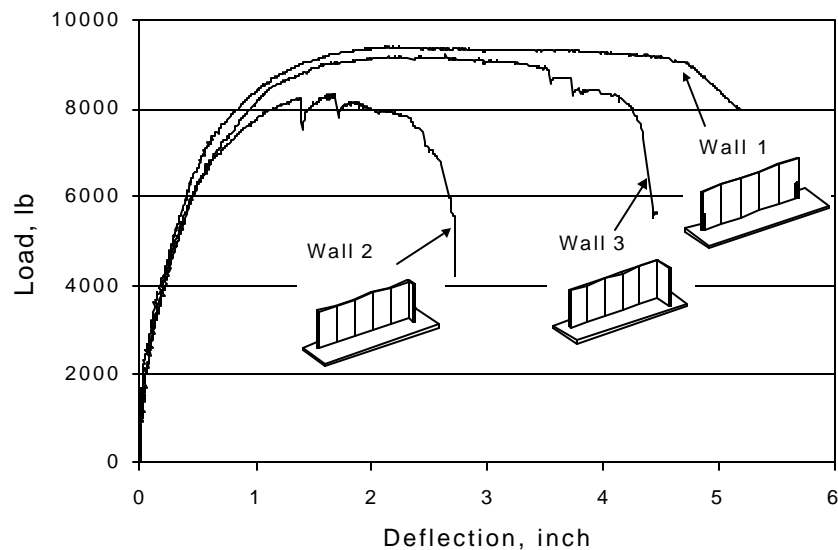


FIGURE 4
LOAD - DEFLECTION RELATIONSHIPS FOR BOLTED WALLS WITHOUT PERFORATIONS

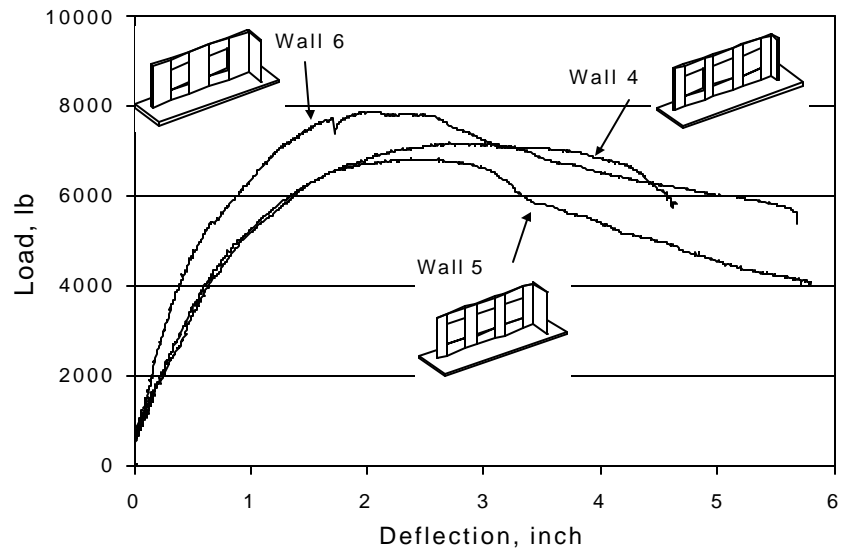


FIGURE 5
LOAD - DEFLECTION RELATIONSHIPS FOR BOLTED WALLS WITH PERFORATIONS

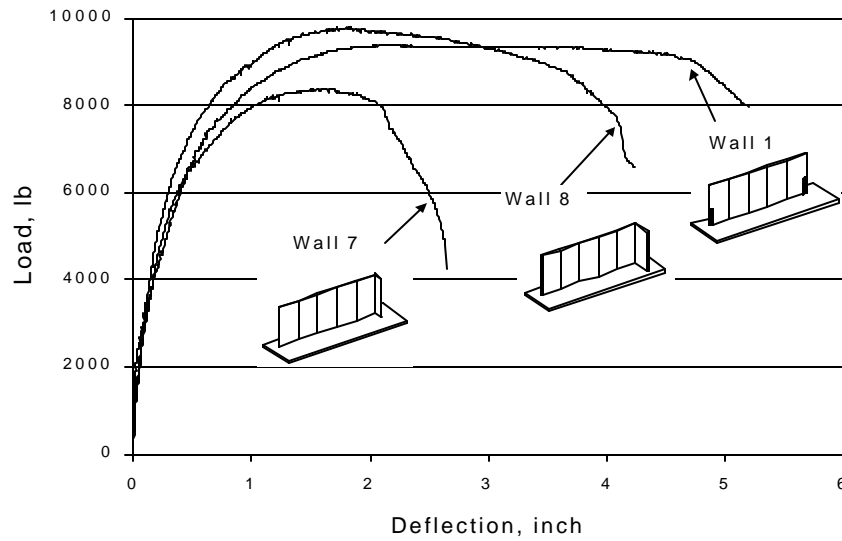


FIGURE 6
LOAD - DEFLECTION RELATIONSHIPS FOR NAILED WALLS WITHOUT PERFORATIONS
(WALL 1 IS INCLUDED FOR COMPARISON)

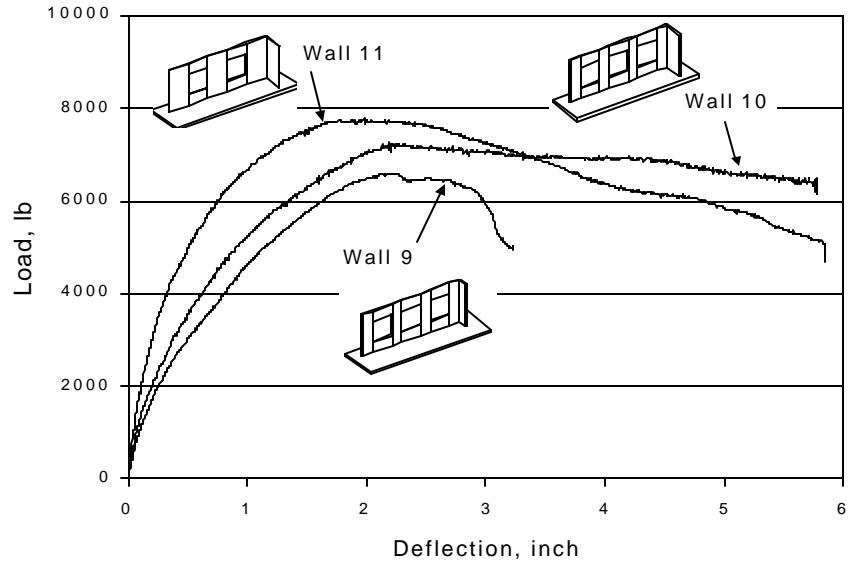


FIGURE 7
LOAD - DEFLECTION RELATIONSHIPS FOR NAILED WALLS WITH PERFORATIONS

The moisture content of the studs was in the range between 9 and 14 percent. The moisture content of the bottom plates was in the range between 6 and 10 percent. The average specific gravity of the studs was 0.49 (COV = 8.0 percent), and the average specific gravity of the bottom and top plates was 0.43 (COV = 15.1 percent).

TABLE 5
PERFORMANCE PARAMETERS OF BOLTED SHEAR WALLS

Parameter	Units	Wall1 r = 1.0 HD	Wall2 r = 1.0 2-ft corner	Wall3 r = 1.0 4-ft corner	Wall4 r = 0.57 2-ft corner	Wall5 r = 0.57 4-ft corner	Wall6 r = 0.75 4-ft corner
Peak load, P_{peak}	lb	9,400	8,359	9,226	7,197	6,849	7,902
Drift at peak load, Δ_{peak}	inch	2.117	1.638	2.641	2.704	2.606	2.047
Uplift at peak load	inch	0.301	1.155	1.106	0.898	0.555	0.896
Yield load, P_{yield}	lb	8,826	7,501	8,549	6,615	6,213	7,010
Drift at yield load, Δ_{yield}	inch	0.347	0.322	0.438	0.889	0.904	0.611
Uplift at yield load	inch	0.212	0.574	0.564	0.531	0.324	0.467
Proportional limit, $0.4P_{max}$	lb	3,760	3,344	3,690	2,879	2,740	3,161
Drift at prop. limit, $\Delta@0.4P_{max}$	inch	0.148	0.144	0.189	0.387	0.399	0.275
Uplift at proportional limit	inch	0.039	0.089	0.050	0.084	0.069	0.072
Failure load or $0.8P_{max}$	lb	7,520	6,688	7,381	5,757	5,479	6,321
Drift at failure, $\Delta_{failure}$	inch	5.355	2.618	4.354	4.615	3.928	4.368
Uplift at failure	inch	0.531	2.486	2.393	2.128	0.686	1.468
Elastic stiffness, K_1	lb/inch	25,426	23,276	19,536	7,441	6,875	11,479
Stiffness at $\Delta=0.1$ inch, K_2	lb/inch	23,756	22,545	20,667	9,527	8,301	10,366
Ductility ratio 1, $\Delta_{peak}/\Delta_{yield}$		6.099	5.082	6.034	3.042	2.884	3.352
Ductility ratio 2, $\Delta_{failure}/\Delta_{yield}$		15.426	8.123	9.950	5.191	4.346	7.152
Toughness of failure index, $\Delta_{failure}/\Delta_{peak}$		2.529	1.598	1.649	1.707	1.507	2.133
Work until failure	lb-inch	45,730	18,427	35,351	27,589	21,597	28,476

TABLE 6
PERFORMANCE PARAMETERS OF NAILED SHEAR WALLS

Parameter	Units	Wall 7	Wall 8	Wall 9	Wall 10	Wall 11
		r = 1.0 2-ft corner	r = 1.0 4-ft corner	r = 0.57 2-ft corner	r = 0.57 4-ft corner	r = 0.75 4-ft corner
Peak load, P_{peak}	lb	8,393	9,791	6,593	7,273	7,798
Drift at peak load, Δ_{peak}	inch	1.615	1.803	2.189	2.194	1.978
Uplift at peak load	inch	1.167	0.834	0.693	0.538	0.618
Yield load, P_{yield}	lb	7,620	8,992	5,835	6,622	6,963
Drift at yield load, Δ_{yield}	inch	0.288	0.316	0.880	0.821	0.469
Uplift at yield load	inch	0.513	0.458	0.406	0.398	0.341
Proportional limit, $0.4P_{max}$	lb	3,357	3,916	2,637	2,909	3,119
Drift at prop. limit, $\Delta@0.4P_{max}$	inch	0.127	0.137	0.398	0.361	0.210
Uplift at proportional limit	inch	0.057	0.056	0.061	0.059	0.043
Failure load or $0.8P_{max}$	lb	6,714	7,833	5,274	5,818	6,238
Drift at failure, $\Delta_{failure}$	inch	2.355	4.047	3.101	5.768	4.218
Uplift at failure	inch	2.268	2.129	1.685	1.331	1.079
Elastic stiffness, K_1	lb/inch	26,481	28,499	6,631	8,063	14,860
Stiffness at $\Delta=0.1$ inch, K_2	lb/inch	28,370	29,913	9,863	11,934	17,841
Ductility ratio 1, $\Delta_{peak}/\Delta_{yield}$		5.612	5.715	2.487	2.672	4.223
Ductility ratio 2, $\Delta_{failure}/\Delta_{yield}$		8.183	12.826	3.524	7.024	9.002
Toughness of failure index, $\Delta_{failure}/\Delta_{peak}$		1.458	2.244	1.417	2.629	2.132
Work until failure	lb-inch	16,848	34,968	15,530	35,476	27,739

5.2 Failure Modes

The failure modes of all wall specimens were associated with a failure or degradation of the components at the uplifting end of the wall. The failure modes of the bolted walls varied and, with the exception of Wall 1, involved degradation of the bottom plate and/or sheathing nails along the bottom plate at the first wall panel (Table 7 and Figure 9). Wall 1 failed due to sheathing nails pulling out of the framing members accompanied with separation of the top plate from the first stud. All five sheathing panels engaged in rotation and developed high shear resistance. The quality of the bottom plate in the vicinity of the first bolt governed the failure mode of walls with corner restraints. There was no apparent correlation between the wall configurations and failure modes. Placing the first bolt closer to the corner would decrease the moment arm and minimize the risk of the parallel-to-grain (weak axis) bending failure mode of the bottom plate. To prevent the cross-grain bending failure of the bottom plate a stiff square washer could have been used with the end anchor bolt. Appendix B compares parallel-to-grain and cross-grain failure modes of the bottom plate.

**TABLE 7
FAILURE MODES
(Bolted Walls)**

Wall #	Failure mode
Wall 1	Bottom plate did not fail, top plate separated from the end stud with the sheathing nail failure at top of the first panel
Wall 2	Bottom plate failed in parallel-to-grain, weak-axis bending
Wall 3	Bottom plate failed in parallel-to-grain, weak-axis bending
Wall 4	Bottom plate did not fail, the first panel separated from the bottom plate
Wall 5	Bottom plate did not fail, the first panel separated from the bottom plate
Wall 6	Bottom plate failed in cross-grain bending (Figure 9)

The nailed walls failed due to withdrawal of the bottom plate nails from the platform. The separation of the bottom plate from the platform led to rigid body rotation of the wall. The location of the effective pivot point of the bottom plate varied for walls with different configurations. For example, the bottom plate pivot point of Wall 7, which was fully sheathed and restrained with 2-foot corner, was approximately 48 inches from the loaded corner near capacity level (Figure 8.a). The bottom plate pivot point of Wall 10, which had three openings and the 24 inch first panel restrained with a 4-foot corner, was approximately 24 inches from the loaded corner near capacity level (Figure 8.b).



a. Wall 7



b. Wall 10

**FIGURE 8
RIGID BODY ROTATION OF THE LOADED END OF NAILED WALLS**

5.3 Corner Return Response

Failure of each wall was accompanied with a degradation of the corner return. The corner returns of the bolted walls failed due to separation of the sheathing panel from the bottom plate. The nails along the bottom plate yielded and either pulled out of the wood or tore through the edge of the panel (Figure 9). The pull-out failure mode prevailed in most cases. The nail connections around the remaining perimeter of the corner panel showed lack of degradation.



FIGURE 9
CORNER RETURN FAILURE
(Wall 6)

Three idealized response levels of the sheathing nails along the bottom plate of the corner are modeled in Figure 10: (1) all nails within elastic performance, (2) nails enter plastic performance, and (3) all nails yield. The shear walls reached their capacity at the third level. These observations were valid for both 2-foot and 4-foot corner returns. Therefore, the effective width of the corner resisting the uplift force near the wall capacity was equal to the width of the corner.

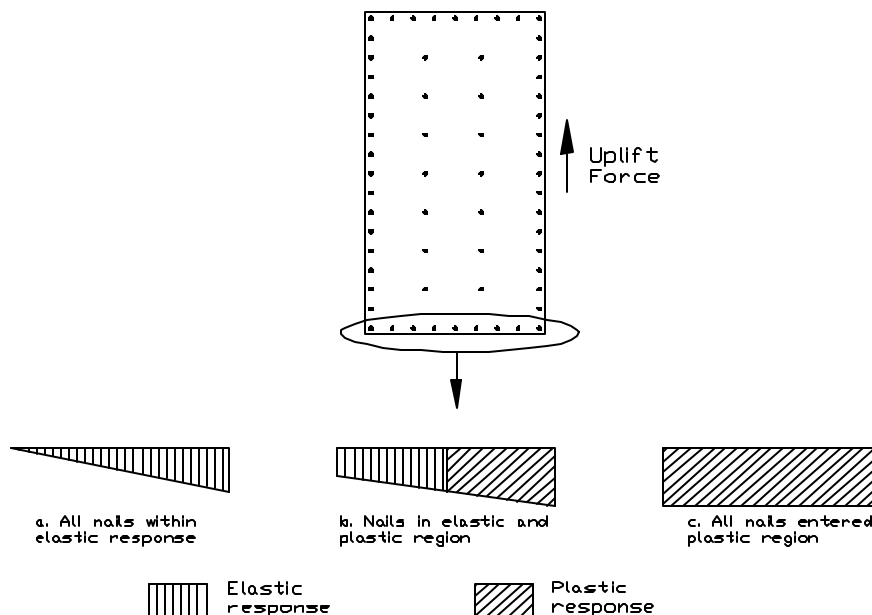


FIGURE 10
RESPONSE OF SHEATHING NAILS ALONG THE BOTTOM PLATE OF A CORNER

The corner returns of the nailed walls failed in different modes. The corner of Wall 7 failed similarly to the corners of the bolted walls. The corners of Walls 8 and 9 failed due to withdrawal of the bottom plate nails from the platform. The corners of Walls 10 and 11 failed

due to partial withdrawal of the bottom nails and pull-out of the sheathing nails along the bottom plate. It should be noted that walls with stronger sheathing nails (i.e., higher shear capacity) would develop higher uplift forces which may have to be offset by an enhanced bottom plate nailing schedule.

The walls without perforations and restrained with the 4-foot corners showed higher capacity and ductility characteristics when compared to the walls restrained with the 2-foot corners. However, an effect of the corner width on the elastic stiffness was not evident. The perforated shear walls showed little correlation between the corner width and the wall capacity and elastic stiffness. The ductility parameters of the perforated walls were improved by using 4-foot corners with the exception of Wall 5.

5.4 Effect of the Bottom Plate Anchorage Methods

Walls with the same opening configurations but with different bottom plate anchorage methods exhibited similar shear capacities with the differences between 0.4 to 8.4 percent. Elastic stiffness of the nailed walls was typically higher than the bolted walls. Wall 8 reached the highest capacity and elastic stiffness among all walls including Wall 1. Because the end stud of Wall 8 was not rigidly secured to the platform, it did not separate from the top plate as in Wall 1. At the same time, the anchorage provided by the corner return was sufficient for the wall to develop shear resistance comparable to the wall with a hold-down (Wall 1).

The change in the anchorage method affected the failure modes as discussed in the previous section. Both nails and bolts effectively resisted the shear force incoming from the wall with the maximum slip between the bottom plate and the platform of 0.10 inch and 0.26 inch, respectively. The increased slip of the bolted walls was likely due to the drilling imperfections of the bolt holes.

Table 8 summarizes the anchor bolt tension forces. Tension in the hold-down of Wall 1 did not exceed 1,585 lb. Ignoring the contribution of the framing nails used to attach the top plate to studs, the maximum uplift force for walls with properly sized hold-downs is equal to the total lateral resistance of the sheathing nails along the first stud of the wall. Because the corner panel is attached to the first stud in the same manner as the wall panel, the same force can be transferred from the main wall into the corner. Analysis of the tension forces demonstrates that the main wall and corner anchor bolts can experience loads of similar magnitudes. For example, the first corner anchor bolt of Walls 3, 4, and 5 resisted higher tension forces at the proportional limit than the first bolt in the main wall. For 4-foot corners, the second corner anchor bolt experienced lower forces at the proportional and yield performance levels as compared to the first corner bolt, whereas the second corner bolt approached or exceeded the first corner bolt for the peak and failure performance levels.

**TABLE 8
SUMMARY OF ANCHOR BOLT LOADS¹**

Wall 1				
	Hold-down bolt, lb	First anchor bolt, lb	First corner bolt, lb	Second corner bolt, lb
Tension @ Peak load	1,530	493	-	-
Tension @ Yield load	1,444	450	-	-
Tension @ Proportional limit	377	181	-	-
Tension @ Failure load	1,585	577	-	-
Wall 2				
	Hold-down bolt, lb	First anchor bolt, lb	First corner bolt, lb	Second corner bolt, lb
Tension @ Peak load	-	1,153	997	-
Tension @ Yield load	-	1,327	687	-
Tension @ Proportional limit	-	603	107	-
Tension @ Failure load	-	690	108	-
Wall 3				
	Hold-down bolt, lb	First anchor bolt, lb	First corner bolt, lb	Second corner bolt, lb
Tension @ Peak load	-	1,544	1052	785
Tension @ Yield load	-	1,333	1292	565
Tension @ Proportional limit	-	444	521	69
Tension @ Failure load	-	747	49	576
Wall 4				
	Hold-down bolt, lb	First anchor bolt, lb	First corner bolt, lb	Second corner bolt, lb
Tension @ Peak load	-	1566	860	-
Tension @ Yield load	-	1297	1096	-
Tension @ Proportional limit	-	425	509	-
Tension @ Failure load	-	1017	0	-
Wall 5				
	Hold-down bolt, lb	First anchor bolt, lb	First corner bolt, lb	Second corner bolt, lb
Tension @ Peak load	-	1379	1174	873
Tension @ Yield load	-	1133	1248	633
Tension @ Proportional limit	-	438	534	213
Tension @ Failure load	-	1315	1106	953
Wall 6				
	Hold-down bolt, lb	First anchor bolt, lb	First corner bolt, lb	Second corner bolt, lb
Tension @ Peak load	-	1056	650	681
Tension @ Yield load	-	1700 ²	877	499
Tension @ Proportional limit	-	679	571	152
Tension @ Failure load	-	678	320	883

¹Reported values are adjusted to account for pre-loading.

²Actual value was higher because force exceeded the load cell range for a short deflection interval containing the maximum reading.

5.5 Uplift Displacement of the End Stud

As expected, the end stud of Wall 1 showed the least uplift displacement among all walls. However, the top plate of Wall 1 separated from the end stud and this event was not captured by LVDT 3. Figures 11 and 12 show end stud uplift displacement vs. wall deflection curves for bolted and nailed walls, respectively. The graphs indicate that the 4-foot corners provided more effective uplift restraint than the 2-foot corners. In addition, the corners were more effective in restraining the perforated walls that the walls without perforations.

The increased uplift was partially caused by the vertical force component produced by the cylinder upward rotation. This effect was a result of the testing apparatus and contributed to accelerated wall degradation, usually after the peak load. The uplift response of shear walls in an actual building assembly can be further improved by the presence of gravity loads in combination with the corner framing, a condition not considered in this study.

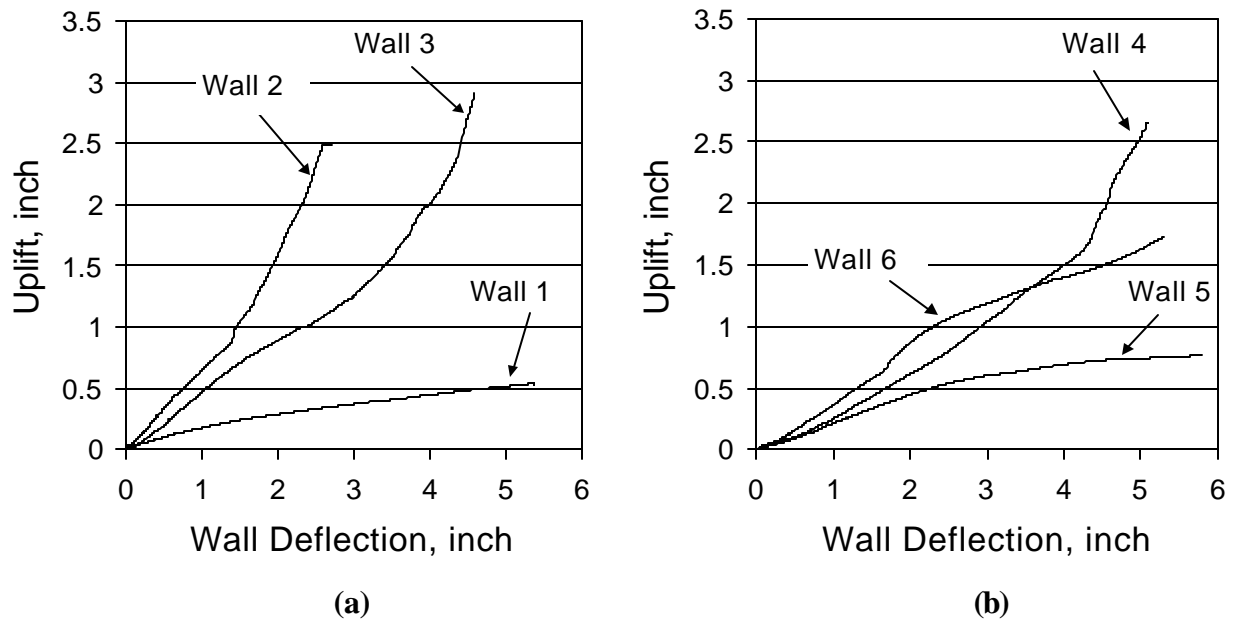


FIGURE 11
WALL UPLIFT DISPLACEMENT VS. WALL DEFLECTION (BOLTED WALLS)

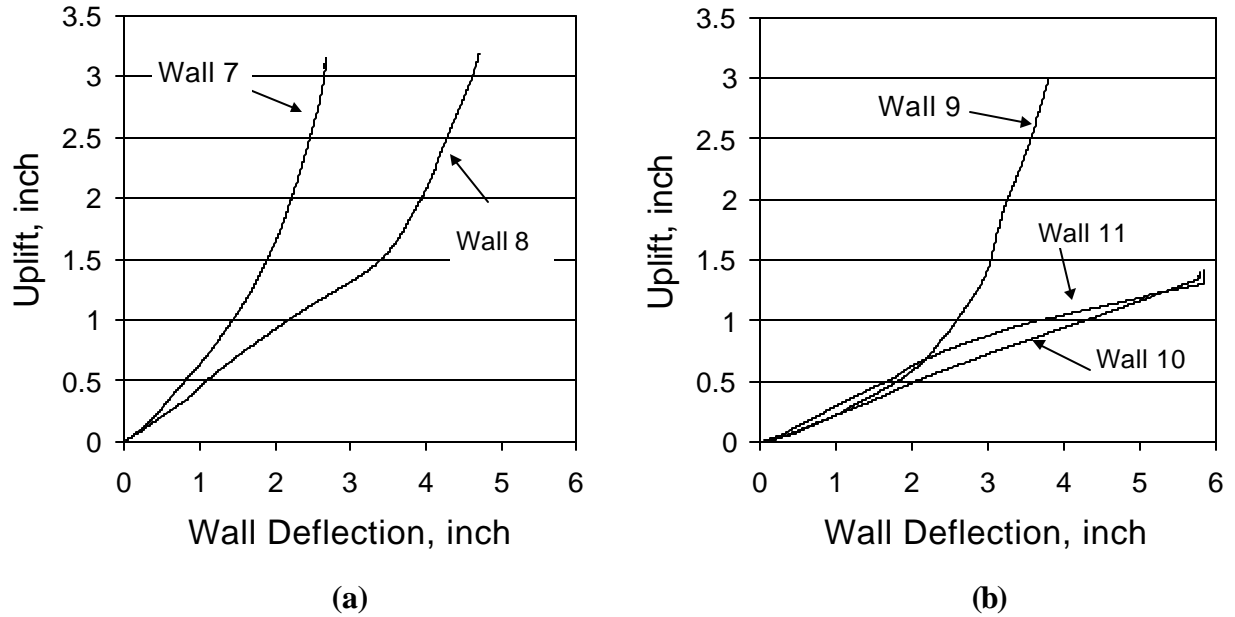


FIGURE 12
WALL UPLIFT DISPLACEMENT VS. WALL DEFLECTION (NAILED WALLS)

5.6 Ductility

The use of corners instead of hold-downs generally decreased the ductility parameters of the shear walls (see Tables 5 and 6). The degree of this effect varied for walls with different configurations. The fully sheathed walls were affected more than the perforated walls. The ductility values showed positive correlation with the corner return width. The corner return provided sufficient uplift resistance for the walls without perforations to approach their maximum possible lateral resistance and elastic stiffness, but the corner was unable to sustain this resistance at large displacements. This effect was attributed to the shift in failure modes at the corner region. The same conclusions were valid for the perforated walls with 2-foot corners. The perforated walls with 4-foot corners showed ductility comparable to that of Wall 1. Ductility values were correlated with the wall uplift response. Therefore, ductility of shear walls in a building assembly can be further improved by decreased uplift, improved corner restraint detailing, or consideration of gravity loads as discussed in Section 5.5.

5.7 Modeling of Shear Walls without Perforations

Two analytical models developed by Ni and Karacabeyli [2] are used to estimate capacity of fully sheathed shear walls with corner restraints. The first model is referred to as mechanics-based (Equation (9)), and the second as empirical (Equation (12)). Because the wall uplift resistance is provided by the sheathing nails along the bottom plate at the corner, the uplift restraint effect, ϕ , is a function of the number and capacity of these nails. Based on the conclusions drawn in Section 5.3, the maximum restraining force develops when all nails along the corner bottom plate yield (Figure 10.c). Therefore, the uplift restraint factor can be determined using Equation (17).

$$\phi = \frac{M_R C_{NR}}{M_S C_{NS}} \quad (17)$$

where:

- M_R = number of nails along the bottom plate of the corner return;
- C_{NR} = capacity of a single nail along the bottom plate;
- M_S = number of nails along the end stud of the wall; and,
- C_{NS} = capacity of a single nail along the end stud.

In Equation (17) it is assumed that the bottom plate bending failure modes that can occur in the bolted walls are prevented (see Appendix B for details) and that the bottom plate to foundation/floor connection is not the weak link. The formulation for the nailed walls should also incorporate the withdrawal failure mode of the nails that secure the corner to the platform. In general, the numerator in Equation (17) should be the minimum value between all possible failure modes.

The ratio, η (Equation (18)), of the nail capacity along the bottom plate to the nail capacity along the end stud depends on the edge distance of the connection and interaction effect between the edge distance and nail diameter.

$$\eta = \frac{C_{NR}}{C_{NS}} \quad (18)$$

Assuming that the nail spacing is constant around the perimeter of the panels, the ratio, β , of the number of nails along the corner bottom plate to the number of nails along the end stud is conservatively expressed with Equation (19). Therefore, β is equal to inverse aspect ratio of the corner return.

$$\beta = \frac{M_R}{M_S} \cong \frac{B}{H} = \frac{1}{\gamma_R} \quad (19)$$

where:

- B = width of the corner return;
- H = height of the wall; and,
- γ_R = aspect ratio of the corner return.

Using Equations (18) and (19) with Equation (17), the uplift restraint factor is a function of the corner geometry and nail capacity as affected by edge distance (Equation (20)).

$$\phi = \frac{\eta}{\gamma_R} \quad (20)$$

For the sheathing nails with small diameter (0.113 inch) and an edge distance of 3/4 inch, η is assumed to be unity and Equation (20) is simplified (Equation (21)).

$$\phi = \frac{1}{\gamma_R} \quad (21)$$

Based on the discussion from the previous section, the effective width of the corner return is equal to the width of the corner panel. The uplift restraint factor is limited to a corner width of 2 feet or 4 feet as tested in this study (Equation (22)).

$$\phi = \frac{1}{\gamma_R} \leq 0.5 \quad (22)$$

Table 9 and Figure 13 compare experimental and analytical results. The wall aspect ratio, γ , is a constant 0.4 for all walls. The empirical model shows better correlation with experimental results than the mechanics-based model. Both models provide conservative estimates. The error for the empirical model ranges between 3 and 9 percent, whereas the error for the mechanics-based model ranges between 14 and 19 percent. The models follow the general trend of the

experimental results that show decrease in the wall capacity with decrease of the restraining force. Because of the low aspect ratio of the walls and relative effectiveness of the corner returns, the decrease in restraining force had minimal effect (<12 percent) on the capacity.

In multi-story construction, if a strap is used to tie the top plate to the end stud or the end stud is strapped to the second floor framing, the uplift force can be higher than the force found by summation the forces resisted by the nails along the end stud. Therefore, the method used to compute the restraint effect, ϕ , should be adjusted for these loading conditions as appropriate for design purposes.

TABLE 9
COMPARISON OF ANALYTICAL AND EXPERIMENTAL RESULTS

Wall #	Restraint Type	$j = g_R$	a , Experim.	a , Mechanics- Based Model	Error, %	a , Empirical Model	Error, %
Wall 1 ¹	HD bracket	1.00	1.000	1.000		1.000	
Wall 2	2 foot corner	0.25	0.889	0.766	14	0.856	4
Wall 3	4 foot corner	0.50	0.982	0.849	14	0.952	3
Wall 7	2 foot corner	0.25	0.893	0.766	14	0.856	4
Wall 8	4 foot corner	0.50	1.042	0.849	19	0.952	9

¹Reference wall.

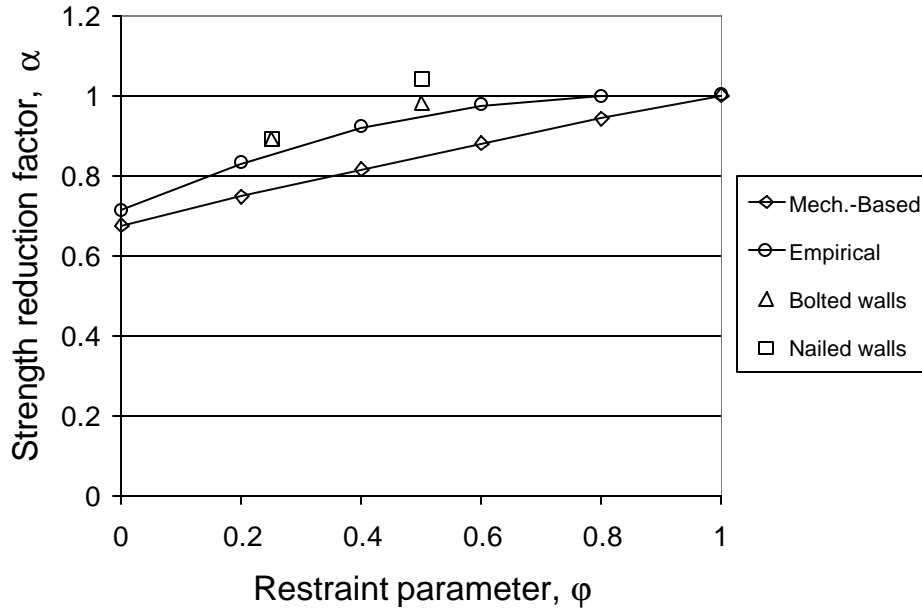


FIGURE 13
COMPARISON OF EXPERIMENTAL DATA FOR WALLS WITHOUT PERFORATIONS WITH THE ANALYTICAL MODELS

5.8 Modeling of Perforated Shear Walls

Perforations had a similar effect on bolted and nailed walls. The area of perforations was negatively correlated with the wall capacity and elastic stiffness. Perforations had greater influence on the elastic stiffness than on the peak load. As expected, the unit shear calculated based on the total wall length decreased as the sheathing area ratio decreased (Table 10). However, the unit shear calculated based on the length of the braced wall panels increased by up to 93 percent (Wall 10) as the sheathing area ratio decreased. Therefore, the components above and below windows contributed to the shear resistance of the wall and should not be ignored from the analysis. Thus, the segmented shear wall method misrepresents the response of this type of wall construction at the capacity performance. The wall components above and below windows restricted rotation of the braced wall panels through contact stress as depicted in Figure 14. This contact stress resulted in development of a counteracting force couple that opposed the panel rotation caused by racking of the wall. The contribution of this force couple was governed by the crushing strength of the OSB panels and resistance of the sheathing nails around the area of contact. Because interference between the wall panels occurred beyond the proportional limit, it did not affect the elastic stiffness of the walls. Based on the visual observations, the components above and below windows showed minimal rotation relative to the framing members.

**TABLE 10
UNIT SHEAR VALUES**

Bolted Walls							
Parameter	Units	Wall1 r = 1.0	Wall2 r = 1.0	Wall3 r = 1.0	Wall4 r = 0.57	Wall5 r = 0.57	Wall6 r = 0.75
Unit shear (Braced Wall Line)	lb/ft	470	418	461	360	342	395
Unit shear (Braced Wall Panels)	lb/ft	470	418	461	900	856	658
Nailed Walls							
Parameter	Units	Wall 7 r = 1.0	Wall 8 r = 1.0	Wall 9 r = 0.57	Wall 10 r = 0.57	Wall 11 r = 0.75	
Unit shear (Braced Wall Line)	lb/ft	420	490	330	364	390	
Unit shear (Braced Wall Panels)	lb/ft	420	490	824	909	650	

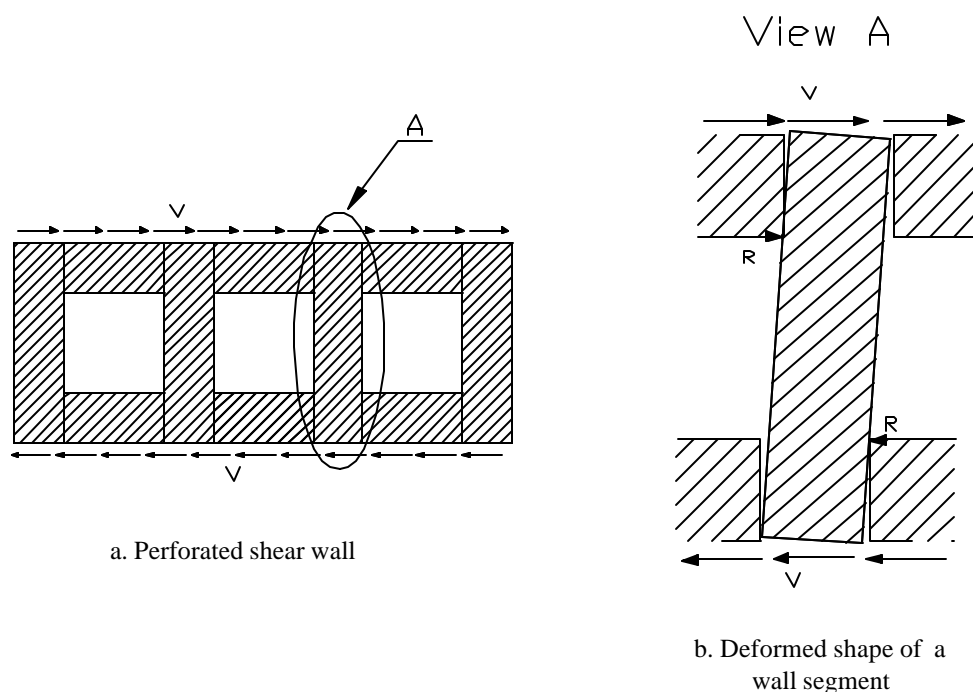


**FIGURE 14
EFFECT OF COMPONENTS ABOVE AND BELOW WINDOWS**

Table 11 and Figures 15 and 16 compare the experimental wall capacities with the predictions of the PSW method. The alternative equation (Equation (3)) is also examined. The walls are organized in four groups so that each group includes walls with the same anchorage method and corner return. The wall without perforations is used as a baseline for the remaining walls of the same group. The PSW method considerably underestimated capacities of the perforated walls with the error up to 64 percent (Wall 4). The lack of door-type openings contributed to the overly conservative predictions of the PSW method in this study. The wall components below window openings restricted rigid body rotation of the adjacent braced wall panels allowing them to

develop substantial shear resistance. The alternative equation provided more accurate results with the maximum conservative error of 54 percent (Wall 4).

TABLE 11
COMPARISON OF EXPERIMENTAL AND ESTIMATED (PSW METHOD) SHEAR WALL CAPACITY

Group ² #	Wall #	r	Experim., lb	PSWM		Alternative Eq. (3)	
				lb	Error, %	lb	Error, %
I	Wall 2 ¹	1.00	8,359	8,359	-	8,359	-
	Wall 4	0.57	7,197	2,562	64	3,332	54
II	Wall 3 ¹	1.00	9,226	9,226	-	9,226	-
	Wall 5	0.57	6,849	2,827	59	3,678	46
	Wall 6	0.75	7,902	4,613	42	5,536	30
III	Wall 7 ¹	1.00	8,393	8,393	-	8,393	-
	Wall 9	0.57	6,593	2,572	61	3,345	49
IV	Wall 8 ¹	1.00	9,791	9,791	-	9,791	-
	Wall 10	0.57	7,273	3,000	59	3,903	46
	Wall 11	0.75	7,798	4,895	37	5,874	25

¹Reference wall for the corresponding group.

²Groups are defined in Figures 15 and 16.

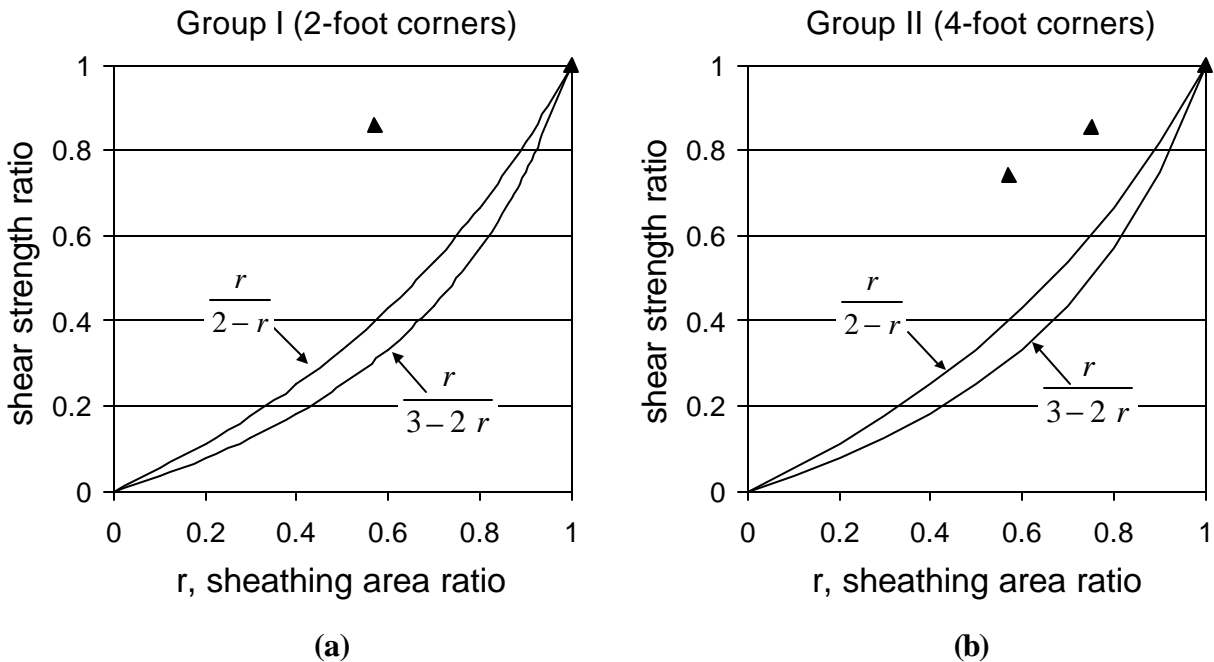


FIGURE 15
COMPARISON OF EXPERIMENTAL AND PREDICTED (PSW METHOD)
SHEAR WALL CAPACITY (BOLTED WALLS)

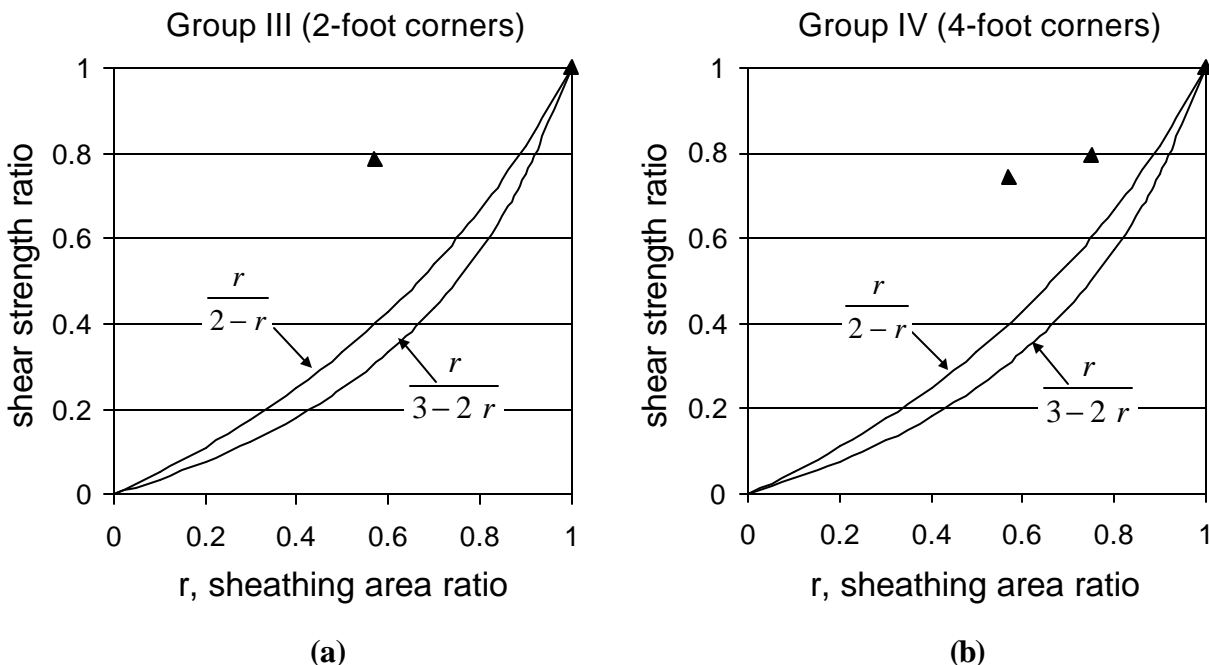


FIGURE 16
COMPARISON OF EXPERIMENTAL AND PREDICTED (PSW METHOD)
SHEAR WALL CAPACITY (NAILED WALLS)

Table 12 and Figures 17 and 18 compare experimental and predicted (PSW method) shear wall stiffnesses. The stiffness at the deflection of 0.1 inch (K_2 - see Tables 5 and 6) was used in the comparison. The PSW method showed good agreement with test results. The conservative error was between 1 (Wall 6) and 28 (Wall 4) percent. Therefore, the PSW method was better correlated with the elastic performance than capacity performance for the perforated walls restrained with corners. The experimental results oscillated around the line predicted using the alternative equation with the maximum error (over-estimate) of 20 percent (Wall 6).

TABLE 12
COMPARISON OF EXPERIMENTAL AND ESTIMATED (PSW METHOD)
SHEAR WALL STIFFNESSES

Group ² #	Wall #	r	Experim., lb/in	PSWM		Alternative Eq. (3)	
				lb/in	Error, %	lb/in	Error, %
I	Wall 2 ¹	1.00	22,545	22,545	-	22,545	-
	Wall 4	0.57	9,527	6,909	28	8,986	6
II	Wall 3 ¹	1.00	20,667	20,667	-	20,667	-
	Wall 5	0.57	8,301	6,333	24	8,238	1
	Wall 6	0.75	10,366	10,334	1	12,400	-20
III	Wall 7 ¹	1.00	28,370	28,370	-	28,370	-
	Wall 9	0.57	9,863	8,694	12	11,308	-15
IV	Wall 8 ¹	1.00	29,913	29,913	-	29,913	-
	Wall 10	0.57	11,934	9,167	23	11,923	1
	Wall 11	0.75	17,841	14,956	16	17,948	-1

¹Reference wall for the corresponding group.

²Groups are defined in Figures 17 and 18.

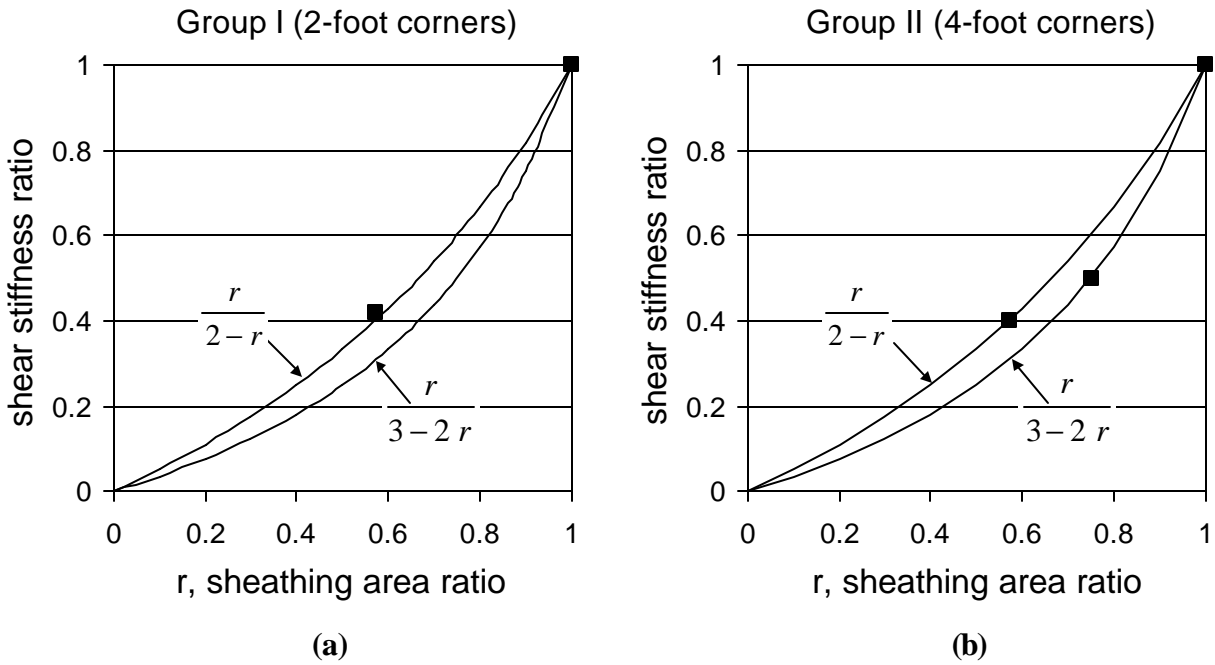


FIGURE 17
COMPARISON OF EXPERIMENTAL AND PREDICTED (PSW METHOD)
SHEAR WALL STIFFNESS AT 0.1 INCH DEFLECTION (BOLTED WALLS)

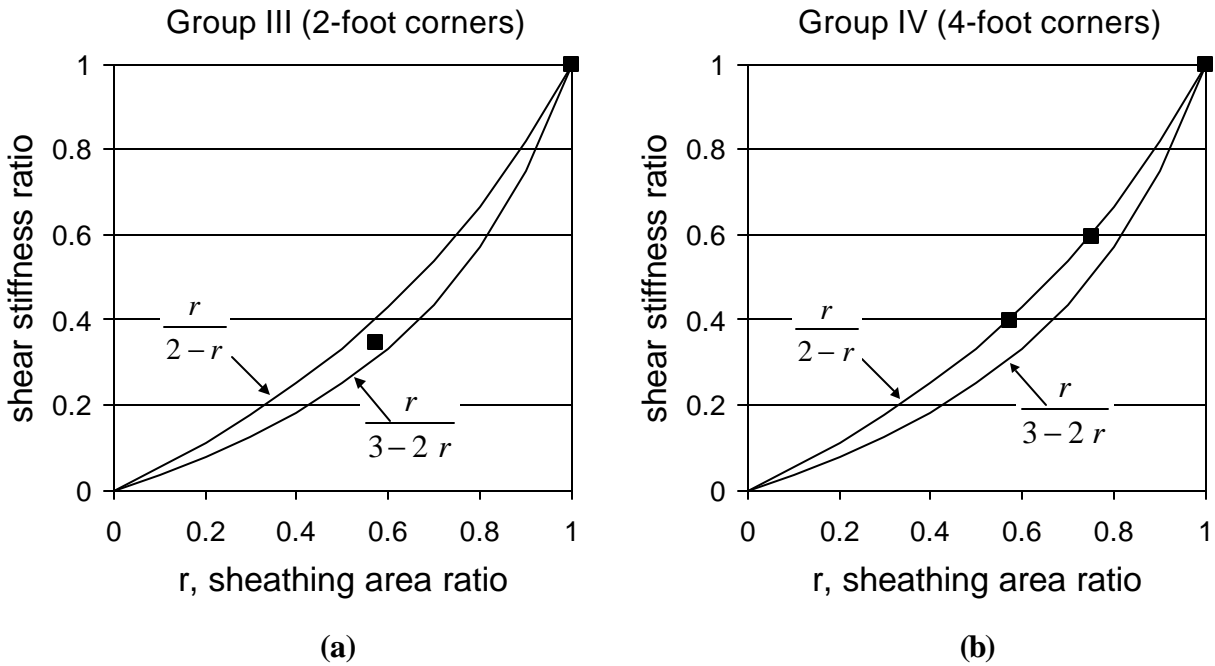


FIGURE 18
COMPARISON OF EXPERIMENTAL AND PREDICTED (PSW METHOD)
SHEAR WALL STIFFNESS AT 0.1 INCH DEFLECTION (NAILED WALLS)

In light of the above discussion, the PSW method may have limited applicability to the conventional shear walls restrained by corner framing. In addition to underestimating the wall capacity, the PSW method requires a baseline resistance for each set of anchorage conditions.

The design method proposed by Ni et al. [3] is compared with test results. The hold-down modification factor, J_{hd} , is calculated using Equations (5) and (22) for the first braced wall panel and it is assumed to be unity for the remaining braced wall panels. The modification factor for wall components is calculated using Equation (7). As shown in Table 13, this method provides more accurate estimates than the PSW method with the maximum conservative error of 30 percent (Wall 4).

TABLE 13
COMPARISON OF EXPERIMENTAL AND ESTIMATED
(FORINTEK METHOD) SHEAR WALL CAPACITY

Wall #	Experimental Capacity, lb	Predicted Capacity, lb	Error, %
Wall 1 ¹	9,400	9,400	-
Wall 2	8,359	8,043	4
Wall 3	9,226	8,952	3
Wall 4	7,197	5,050	30
Wall 5	6,849	5,327	22
Wall 6	7,902	6,517	18
Wall 7	8,393	8,043	4
Wall 8	9,791	8,952	9
Wall 9	6,593	5,050	23
Wall 10	7,273	5,327	27
Wall 11	7,798	6,517	16

¹Reference wall.

6. Summary and Conclusions

The following conclusions are organized in three groups to answer the corresponding project objectives (see Introduction). Each conclusion is accompanied with a summary.

(1)

- The elastic stiffness of conventional shear walls restrained with corners was equivalent to that of an engineered shear wall. Conventional shear walls restrained with the 4-foot corners approached or exceeded capacity of an engineered shear wall.
- The use of corner returns instead of hold-downs decreased the wall ductility characteristics. This reduction was the result of the changes in the failure modes.
- Separation of the sheathing panel from the bottom plate near the corner and bending failure of the bottom plate were the typical failure modes for the bolted walls. Withdrawal of the bottom plate nails from the platform was the typical failure mode for the nailed walls.
- The failure of each wall was accompanied with an uplift failure of the corner return. The corners provided the uplift resistance through the nails along the bottom plate. The remaining sheathing nails of the corner panel showed lack of degradation.

(2)

- The corners enhanced the performance of conventional wood shear walls by providing partial overturning restraint. The uplift force resisted by the corner was equivalent to the uplift force at the loaded end of the shear wall.
- The fully sheathed walls with the 4-foot corners reached higher capacities and showed larger ductility characteristics than the fully sheathed walls with the 2-foot corners.
- The perforated walls ($r = 0.57$ and $r = 0.75$) restrained with corners showed higher ductility as compared to the walls without perforations. The corner width (2 feet vs. 4 feet) showed lack of influence on the elastic stiffness.
- The effective corner width that engaged in the uplift resistance was equal to the width of the corner panel.

(3)

- The PSW method considerably underestimated capacity of the perforated shear walls restrained with corner returns. The stiffness of the perforated walls predicted using the PSW method showed good agreement with the experimental data. Therefore, the PSW method showed limited applicability for the perforated wood shear walls with partial restraints.
- The method proposed by Ni et al. [3] provided more accurate results than the PSW method and is more suitable for the analysis of conventional shear walls. The mechanics-based and empirical methods developed by Ni and Karacabeyli [3] for modeling the limit state response of shear walls without perforations were in good agreement with test results. The mechanics-based method provided more conservative estimates as compared with the empirical method.
- The overturning resistance provided by the corner was formulated as a function of the corner geometry and sheathing nail capacity. The formulation was further simplified to include only the wall geometry. The derivation was validated using shear walls with an aspect ratio of 0.4.

All walls exhibited overall behavior that is relevant to design applications provided the response is adequately predicted and compared to required load demand with an appropriate factor of safety. Because of the decreased ductility, conventional shear walls should be assigned larger safety margins as opposed to more ductile engineered walls. The discussed methods of shear wall analysis can be readily incorporated into the capacity-based design methodologies that will allow the engineer to design conventionally constructed buildings with known performance. Moreover, these methods of analysis can be used to design economical enhancements for conventional buildings, and to establish comparative performance parameters for innovative methods and materials in housing. Public adoption of the discussed design methods can be facilitated by advancing the knowledge in the field of light-frame wood shear walls through answering the problems formulated in the following section.

7. Recommendations for Future Research

This section identifies future research projects that will provide new insights into the performance of conventional wood shear walls and contribute to the development of improved design methods for wood light-frame structures.

- (1) Walls with lower and higher aspect ratios should be investigated to validate the project conclusions for the wider range of wall geometries.
- (2) Walls with other configurations of perforations including door openings and sheathing area ratios should be examined to expand the scope of this project.
- (3) Tests of three-dimensional assemblies including walls and diaphragms loaded at an oblique angle should be conducted to explore the effect of this loading condition on the corner performance.
- (4) The effect of the gravity loads on the overturning resistance of shear walls with corners should be investigated.
- (5) The effect of longer corners and corners with perforations should be investigated.
- (6) Similar walls with decreased sheathing nail spacing (i.e., higher unit shear capacity) should be investigated.
- (7) Enhanced wall construction details, such as the use of truss plates on corner framing joints and plate washers on anchor bolts should be further explored.
- (8) A comprehensive and accurate design method for walls with various corner or end restraint and load conditions should begin to be formulated for general design applications.

8. References

- [1] ASTM. 1997. Annual Book of ASTM Standards, Volume 04.11, Building Constructions. American Society of Testing and Materials, West Conshohocken, PA.
- [2] Ni, C., and Karacabeyli, E. 2000. Effect of overturning restraint of performance of shear walls. Proceedings of the World Conference on Timber Engineering. Whistler Resort, British Columbia, Canada.
- [3] Ni, C., Karacabeyli, E., and Ceccotti, A. 1998. Design of shear walls with openings under lateral and vertical loads. Paper prepared for PTEC'99, Draft v. 4, December 2.
- [4] Dolan, J., and Heine, C. 1997. Monotonic Tests of Wood Frame Shear Walls with Various Openings and Base Restraint Configurations. Prepared for the NAHB Research Center, Inc. by Virginia Polytechnic Institute and State University, Blacksburg, VA.
- [5] Dolan, J., and Heine, C. 1997. Sequential Phased Displacement Cyclic Tests of Wood Frame Shear Walls with Various Openings and Base Restraint Configurations. Prepared for the NAHB Research Center Inc. by Virginia Polytechnic Institute and State University, Blacksburg, VA.
- [6] Dolan, J., and Heine, C. 1997. Sequential Phased Displacement Tests of Wood Framed Shear Walls with Corners. Prepared for the NAHB Research Center, Inc. by Virginia Polytechnic Institute and State University, Blacksburg, VA.

- [7] Salenikovich, A. J. 2000. The racking performance of light-frame shear walls. Ph.D. dissertation. Virginia Polytechnic Institute and State University, Blacksburg, VA.
- [8] NAHB Research Center, Inc. 1998. The Performance of Perforated Shear Walls with Narrow Wall Segments, Reduced Base Restraint, and Alternative Framing Methods. Prepared for the U.S. Department of Housing and Urban Development and The National Association of Home Builders by the NAHB Research Center, Inc., Upper Marlboro, MD.
- [9] NAHB Research Center, Inc. 1999. Perforated Shear Walls with Conventional and Innovative Base Restraint Connections. Prepared for the U.S. Department of Housing and Urban Development and The National Association of Home Builders by the NAHB Research Center, Inc., Upper Marlboro, MD.
- [10] Sugiyama, H., and Yasumura, M. 1984. Shear Properties of Plywood Sheathed Wall Panels with Openings. Trans. of A.I.J., No. 338. Japan.
- [11] Sugiyama, H., and Matsumoto, T. 1994. Empirical Equations for the Estimation of Racking Strength of a Plywood Sheathed Shear Wall with Openings. Summary of Technical Papers, Annual Meetings, Trans. of A.I.J. Japan.
- [12] Dolan, J., and Johnson, A. 1996. Cyclic and Monotonic Tests of Long Shear Walls with Openings. Prepared for the American Forest & Paper Association by Virginia Polytechnic Institute and State University, Blacksburg, VA.
- [13] Porter, M. L. 1987. Sequential Phase Displacement Procedure for TCCMAR Testing. Proceedings of the Third Meeting of the Joint Technical Coordinating Committee on Masonry Research, US-Japan Coordinated Earthquake Research Program, Tomamu, Japan.
- [14] Thurston S. J. 1993. Report on racking resistance of long sheathed timber framed walls with openings. BRANZ study report NO. 54. Building Research Association of New Zealand, Judgeford, New Zealand.
- [15] Salenikovich, A. J., and Dolan, J. D. 2000. The racking performance of light-frame shear walls with various tie-down restraints. Proceedings of the World Conference on Timber Engineering. Whistler Resort, British Columbia, Canada.
- [16] International Code Council (ICC). 2000. International Building Code for One- and Two-Family Dwellings. ICC, Falls Church, VA.
- [17] National Evaluation Service, Inc. 1996. Report No. NER-272, "Power Driven Staples, Nails, and Allied Fasteners for Use in All Types of Building Construction." Council of American Building Officials, Falls Church, VA.
- [18] Simpson Strong-Tie® Co., Inc. 1999. Catalog C-99. Wood Construction Connectors. Simpson Strong-Tie® Co., Inc., Pleasanton, CA.

- [19] ASTM. 1999. Annual Book of ASTM Standards, Volume 04.10, Wood. American Society of Testing and Materials, West Conshohocken, PA.
- [20] IOtech, Inc. 1996. DaqView™ v. 5.0. IOtech, Inc., Cleveland, Ohio.
- [21] Forest Products Laboratory. 1999. Wood handbook--Wood as an engineering material. Gen. Tech. Rep. FPL-GTR-113. Madison, WI: U.S. Department of Agriculture, Forest Service, Forest Products Laboratory. 463 p.

APPENDIX A

BOTTOM PLATE NAIL WITHDRAWAL TESTS

This appendix reports results of the individual nail withdrawal tests. The withdrawal capacity of 16d short full-round-head bright basic pneumatic nails (3-1/4 inch long x 0.131 inch diameter), which were used to attach the shear wall bottom plate to the platform, was measured. Two types of connections were tested: (i) nail penetrating a 23/32-inch thick OSB subfloor panel (APA rated 24 inches on center) and a 2 x 4 inch nominal SPF board, and (ii) nail penetrating a 23/32-inch thick OSB subfloor panel. Figure A1 shows the test specimen configurations. Ten specimens of each configuration were tested. The tests were conducted according to the ASTM Standard D 1761 "Standard Test Methods for Mechanical Fasteners in Wood" [19] at a constant rate of 0.1 inch/min. The specimens were tested 72 hours after the fabrication to allow for partial stress relaxation. Table A1 summarizes the test results. The moisture content of the SPF board ranged between 9 and 11 percent. The specific gravity of the SPF board was 0.47 (COV = 5.9 percent). The data represent direct withdrawal resistance only, and not combined effects of shear and uplift as would be experienced in a conventional shear wall.

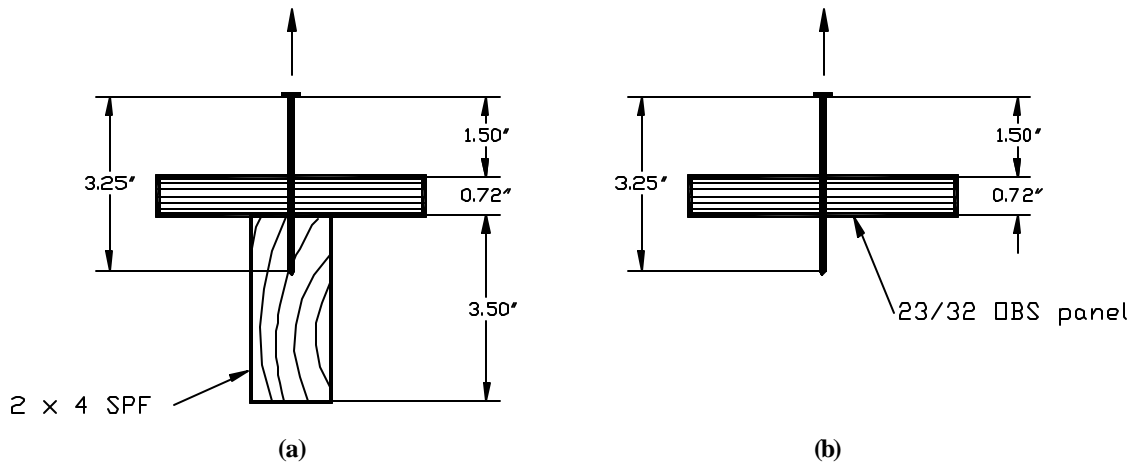


FIGURE A1
SPECIMEN CONFIGURATIONS

TABLE A1
WITHDRAWAL CAPACITY OF INDIVIDUAL NAILS

Specimen configuration	Peak load, lb	Peak load COV, %
OSB panel and 2 x 4 SPF	463	21.4
OSB panel	195	37.3

APPENDIX B

ANALYSIS OF THE FAILURE MODES OF THE SHEAR WALL BOTTOM PLATE

This appendix is intended to explore methods of predicting two possible failure modes of bottom plates for partially restrained wood shear walls attached to the foundation using anchor bolts. The presented analysis makes a series of assumptions regarding both loading conditions and material resistance. Therefore, results of the analysis are for demonstration purposes only and are subject to further refinements.

1. Parallel-to-grain bending

The bottom plate is bolted to a rigid foundation. The distance from the wall corner to the first bolt is 12 inches. It is assumed that the capacity of the sheathing-to-frame nail connection is P . The bottom plate is modeled as a cantilever beam (Figure B1) with a fixed joint at the location of the first bolt. Because the nail spacing is 6 inches, two nails from the first panel and one nail from the corner apply bending moment on the bottom plate. The nails are modeled as point loads. The strength of the framing nails in the end grain of the studs is assumed to be zero.

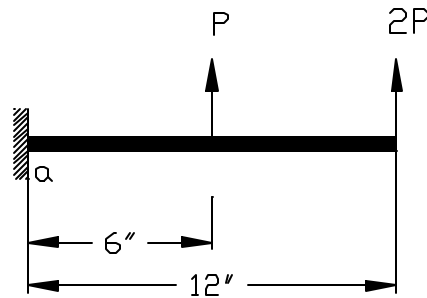


FIGURE B1
PARALLEL-TO-GRAIN BENDING (BOTTOM PLATE WEAK AXIS)

Moment at the fixed joint:

$$M_a = P * 6 + 2P * 12 = 30P \text{ lb-in}$$

Bending stress:

$$\sigma_p = 30P/S = 30P/1.313 = 22.85P \text{ psi}$$

where: $S = bh^2/6 = 3.5 * 1.5^2/6 = 1.313 \text{ in}^3$

2. Cross-grain bending

The bottom plate is modeled as a cantilever beam fixed in the middle of its cross section (Figure B2). The effective length of 6 inches is assumed on the basis of the sheathing nail spacing.

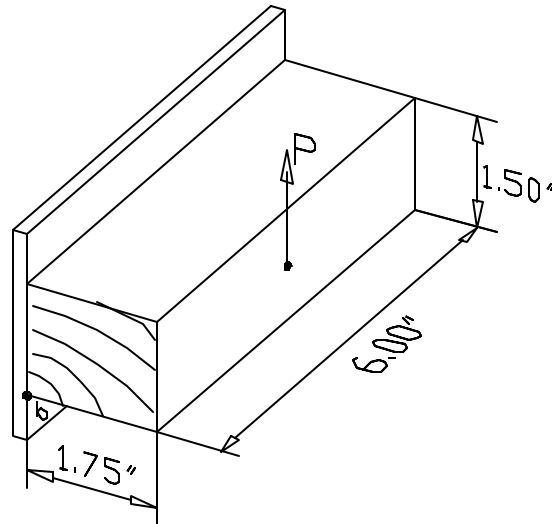


FIGURE B2
BOTTOM PLATE CROSS-GRAIN BENDING

Moment at the fixed joint:

$$M_b = P * 1.75 = 1.75P \text{ lb-in}$$

Bending stress:

$$\sigma_c = 1.75P/S = 0.78P \text{ psi}$$

$$\text{where: } S = bh^2/6 = 6 * 1.5^2/6 = 2.25 \text{ in}^3$$

The ratio of the parallel-to-grain bending stress to cross grain bending stress:

$$\mu = \sigma_p / \sigma_c = 22.85P / 0.78P = 29.3$$

The ratio of the wood strength properties in the corresponding directions varies between wood species. The authors are unaware of the tabulated values for cross-grain bending. Tension perpendicular-to-grain is used instead. Table B1 summarizes the strength properties for selected species from the SPF sawn lumber species combination derived from the clear wood specimen tests as reported in the Wood Handbook [21].

TABLE B1
STRENGTH PROPERTIES FOR THE SPF SAWN LUMBER SPECIES COMBINATION

Species	MOR, psi	Tension perpendicular to grain, psi	Ratio
Engelmann Spruce	9,300	350	26.6
White Spruce	9,400	360	26.1
Balsam Fir	9,200	180	51.1
Lodgepole Pine	9,400	290	32.4
Jack Pine	9,900	420	23.6

The comparison of the load and strength ratios indicates that either failure mode can govern the bottom plate capacity if sufficient uplift load is realized. This conclusion is consistent with findings of this study Table 7. The defects such as knots, drying checks, and splits initiated by nails can influence the failure modes in a different manner. End-grain splits can substantially reduce the cross-grain bending strength. A square washer of 3 x 3 inches can be used with the corner anchor bolts to reduce the moment arm and minimize the risk of this failure mode. Positioning the first bolt closer to the corner can minimize the risk of the parallel-to-grain failure mode.

APPENDIX C

METRIC CONVERSION FACTORS

The following list provides the conversion relationship between U.S. customary units and the International System (SI) units. A complete guide to the SI system and its use can be found in ASTM E 380, Metric Practice.

To convert from to multiply by

Length

inch (in.)	meter (μ)	25.400
inch (in.)	centimeter	2.54
inch (in.)	meter (m)	0.0254
foot (ft)	meter (m)	0.3048
yard (yd)	meter (m)	0.9144
mile (mi)	kilometer (km)	1.6

Area

square foot (sq ft)	square meter (sq m)	0.09290304E
square inch (sq in)	square centimeter (sq cm)	6.452 E
square inch (sq in.)	square meter (sq m)	0.00064516E
square yard (sq yd)	square meter (sq m)	0.8391274
square mile (sq mi)	square kilometer (sq km)	2.6

Volume

cubic inch (cu in.)	cubic centimeter (cu cm)	16.387064
cubic inch (cu in.)	cubic meter (cu m)	0.00001639
cubic foot (cu ft)	cubic meter (cu m)	0.02831685
cubic yard (cu yd)	cubic meter (cu m)	0.7645549
gallon (gal) Can. liquid	liter	4.546
gallon (gal) Can. liquid	cubic meter (cu m)	0.004546
gallon (gal) U.S. liquid*	liter	3.7854118
gallon (gal) U.S. liquid	cubic meter (cu m)	0.00378541
fluid ounce (fl oz)	milliliters (ml)	29.57353
fluid ounce (fl oz)	cubic meter (cu m)	0.00002957

Force

kip (1000 lb)	kilogram (kg)	453.6
kip (1000 lb)	Newton (N)	4,448.222
pound (lb)	kilogram (kg)	0.4535924
pound (lb)	Newton (N)	4.448222

Stress or pressure

kip/sq inch (ksi)	megapascal (Mpa)	6.894757
kip/sq inch (ksi)	kilogram/square centimeter (kg/sq cm)	70.31
pound/sq inch (psi)	kilogram/square centimeter (kg/sq cm)	0.07031
pound/sq inch (psi)	pascal (Pa) **	6,894.757
pound/sq inch (psi)	megapascal (Mpa)	0.00689476
pound/sq foot (psf)	kilogram/square meter (kg/sq m)	4.8824
pound/sq foot (psf)	pascal (Pa)	47.88

To convert from to multiply by

Mass (weight)

pound (lb) avoirdupois	kilogram (kg)	0.4535924
ton, 2000 lb	kilogram (kg)	907.1848
grain	kilogram (kg)	0.0000648

Mass (weight) per length

kip per linear foot (klf)	kilogram per meter (kg/m)	0.001488
pound per linear foot (plf)	kilogram per meter (kg/m)	1.488

Moment

1 foot-pound (ft-lb)	Newton-meter (N-m)	1.356
----------------------	--------------------	-------

Mass per volume (density)

pound per cubic foot (pcf)	kilogram per cubic meter (kg/cu m)	16.01846
pound per cubic yard (lb/cu yd)	kilogram per cubic meter (kg/cu m)	0.5933

Velocity

mile per hour (mph)	kilometer per hour (km/hr)	1.60934
mile per hour (mph)	kilometer per second (km/sec)	0.44704

Temperature

degree Fahrenheit (°F)	degree Celsius (°C)	$t_C = (t_F - 32)/1.8$
degree Fahrenheit (°F)	degree Kelvin (°K)	$t_K = (t_F + 459.7)/1.8$
degree Kelvin (°F)	degree Celsius (°C)	$t_C = (t_K - 32)/1.8$

* One U.S. gallon equals 0.8327 Canadian gallon

** A pascal equals 1000 Newton per square meter.

The prefixes and symbols below are commonly used to form names and symbols of the decimal multiples and submultiples of the SI units.

Multiplication Factor	Prefix	Symbol
1,000,000,000 = 10 ⁹	giga	G
1,000,000 = 10 ⁶	mega	M
1,000 = 10 ³	kilo	k
0.01 = 10 ⁻²	centi	c
0.001 = 10 ⁻³	milli	m
0.000001 = 10 ⁻⁶	micro	μ
0.000000001 = 10 ⁻⁹	nano	n